

RESEARCH ARTICLE | FEBRUARY 16 2024

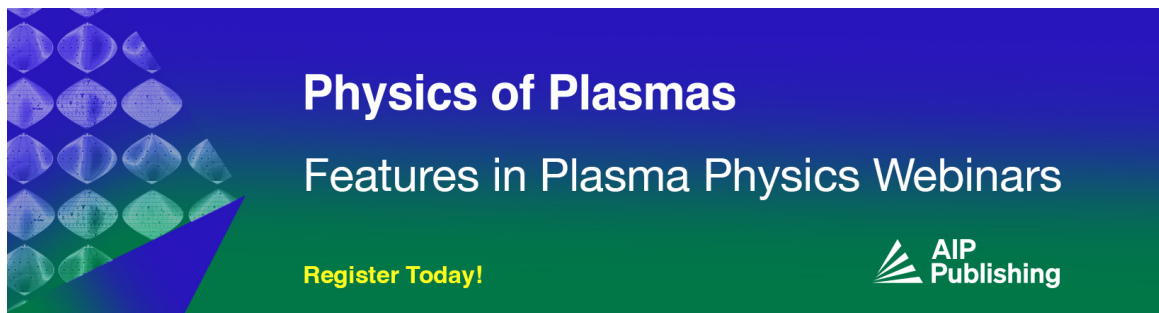
Dynamic evolutions of Bohm sheaths and pre-sheaths

Mitsuo Kono ; Hans L. Pécseli  



Phys. Plasmas 31, 023508 (2024)

<https://doi.org/10.1063/5.0176287>



Physics of Plasmas
Features in Plasma Physics Webinars

Register Today!



Dynamic evolutions of Bohm sheaths and pre-sheaths

Cite as: Phys. Plasmas **31**, 023508 (2024); doi: [10.1063/5.0176287](https://doi.org/10.1063/5.0176287)

Submitted: 12 September 2023 · Accepted: 16 January 2024 ·

Published Online: 16 February 2024





View Online



Export Citation



CrossMark

Mitsuo Kono¹  and Hans L. Pécseli^{2,a)} 

AFFILIATIONS

¹Faculty of Policy Studies, Chuo University, Hachioji, Tokyo 192-0393, Japan

²Department of Physics and Technology, UiT The Arctic University of Norway, N-9037 Tromsø, Norway

^{a)}Also at: Department of Physics, University of Oslo, N-0316 Blindern, Norway. Author to whom correspondence should be addressed: hans.pecseli@fys.uio.no

ABSTRACT

The time evolutions of the Bohm sheath and the related pre-sheath are analyzed as an initial value problem. The standard classical fluid model of a collisionless plasma is used with cold ions and Boltzmann distributed electrons. Numerical solutions of the basic equations show that a stationary plasma sheath itself is established within a few ion plasma periods. It is demonstrated analytically that for infinitely extended homogeneous plasmas in one spatial dimension, the only possible pre-sheath solution is dynamic, giving a steady expansion: no stationary solution exists for this one-dimensional case. The potential and density drops along the dynamic pre-sheath differ notably from the values found for stationary models suggested in the literature. Collisions give only formal changes to the collisionless results, and their substance remains the same in one spatial dimension. Cylindrical and spherical geometries, on the other hand, allow for physically acceptable, fully nonlinear, stationary solutions with analytical results given. These are supported by numerical solutions.

© 2024 Author(s). All article content, except where otherwise noted, is licensed under a Creative Commons Attribution (CC BY) license (<http://creativecommons.org/licenses/by/4.0/>). <https://doi.org/10.1063/5.0176287>

I. INTRODUCTION

When a conducting surface at some externally applied negative potential is embedded in a plasma, it will absorb ions and reflect electrons to form a plasma sheath in the vicinity of the surface. The problem in its basic form is commonly met in laboratory, in industrial plasmas, and also for a number of space plasma applications. Probes used for plasma diagnostics offer a particularly important problem. Ideal collisionless and collision-dominated plasmas represent two limiting cases. The present study is concerned with the classical version of the plasma sheath conditions where a large negative potential is applied to a conducting surface facing a collisionless plasma. Based on the assumption of a stable time-stationary sheath, Bohm's observation¹ states that ions have to arrive at sonic or supersonic velocities at the sheath edge in order to give a stable sheath solution.²⁻⁷ A pre-sheath is necessary for accelerating ions to this velocity. Here, we address a question concerning the length scales of the problem, which can be argued also by dimensional analysis with arguments substantiated in an Appendix A (see also Table 1). The plasma sheath facing the biased surface is characterized by a charge imbalance. For the collisionless case, its width scales with the electron Debye length, while the pre-sheath is quasi-neutral and has no natural characteristic length scale

(such as the electron Debye length), nor any natural timescale (such as the electron or ion plasma periods). Length scales can be imposed through the initial conditions, but step-like or δ -function like conditions have no such built-in scales, but are legitimate initial conditions nonetheless. Without a characteristic length scale, the pre-sheath width is undetermined,⁸ see also Appendix A. This ambiguity is resolved by considering the problem as an initial value problem,^{9,10} where the sheath itself is established almost instantaneously, while the pre-sheath is formed through a steady-state expansion, propagating with the ion sound speed. The characteristic length scale in physical units thus becomes $\mathcal{L}(t) = C_s t$ in terms of the ion sound speed and time t . The analysis is based on exact analytical solutions of the basic equations and supplemented by numerical results. We find the potential and density drops along the dynamic pre-sheath to differ notably from the values found for stationary models. There is a significant difference between static and dynamic pre-sheath conditions.

All ions are lost to the negatively biased terminating conducting plate, and in this sense, the problem has some similarities with expansion of step-like plasma discontinuities¹¹⁻¹³ and plasma expansion into vacuum being a limiting case.¹⁴ The self-similar evolution has been demonstrated also experimentally and numerically.^{13,15,16}

This problem is interesting also in the present context by the self-similar solutions found in certain limits.

Introducing collisions with a frequency μ into the model gives an additional length scale C_s/μ in the model equations. Also, this case has an exact analytical solution, but it turns out that this solution is not accessible from physically acceptable conditions with finite plasma densities.

Problems in higher dimensions with imposed characteristic length scales have different properties. Cylindrically and spherically symmetric conditions can differ from the infinite one-dimensional case by having a natural length scales such as the radius of the conducting surface. These cases are analyzed as well in the present study and exact analytical expressions given for the time-stationary pre-sheath. Introducing collisions in these problems means that they have two competing length scales, the Debye length and the collisional mean free path.

The analytical results are supported by numerical solutions of the basic set of nonlinear equation. For the two- and three-dimensional cases (with cylindrical and spherical symmetries, respectively), these numerical results illustrate how the analytically obtained stationary solutions develop from physically realistic initial conditions. The emphasis of the analysis is on the properties of the pre-sheath and its evolution.

II. BASIC EQUATIONS

The basic analytical model used in much of the following is based on the standard fluid equations for a two-component plasma with cold ions and isothermally Boltzmann distributed electrons at temperature T_e . Multi-component plasmas, in particular also with charged dust particles embedded,¹⁷ can be interesting as well for both industrial and space applications, but these are not considered here

$$\frac{\partial}{\partial t} \mathbf{u} + (\mathbf{u} \cdot \nabla) \mathbf{u} = -\frac{e}{M} \nabla \phi, \quad (1)$$

$$\frac{\partial}{\partial t} n + \nabla \cdot (n\mathbf{u}) = 0, \quad (2)$$

$$\nabla^2 \phi = \frac{e}{\epsilon_0} (n_p e^{e\phi/T_e} - n), \quad (3)$$

where the density and velocity of singly charged ions with mass M are n and \mathbf{u} , the electrostatic potential is ϕ , and T_e is the electron temperature with Boltzmann's constant κ included, while n_p is a reference electron density, which is also the plasma density for unperturbed plasmas with $\phi = 0$. Contributions from an ion pressure term are ignored. For large electron to ion temperature ratios, $T_e/T_i \gg 1$, this approximation is justified. Isothermal ion contributions will not give substantial modification of the results. Adiabatic ion dynamics will give a nonlinear correction, but this will be small for the assumed large temperature ratios. The equations have to be completed by initial and boundary conditions. We assume externally applied negative potentials to a solid surface, which can be planar, cylindrical, or spherical, and consider semi-infinite plasma domains. The conditions (plasma density, plasma potential, and velocity) are taken to be constant at infinity. Numerical results will use large but spatially finite systems.

The set of Eqs. (1)–(3) has its limitations, but has been widely used for discussing the basic properties of sheaths and pre-sheaths. The equations describe, for instance, the low-frequency collisionless dynamics of linear as well as nonlinear ion acoustic waves propagating along the magnetic field lines in Q-machines.¹⁸ For unmagnetized double-plasma

(DP) devices¹⁹ operated at low neutral pressures with $T_e \gg T_i$, it is also possible to ignore collisions for a wide class of low-frequency plasma problems. The assumption of Boltzmann distributed electrons, in particular, is widely used^{3,20–23} in describing low-frequency (below the ion plasma frequency Ω_{pi}) plasma phenomena. The electron inertia terms are ignored in the electron momentum equation, so the electron pressure term is balanced by the electrostatic forces to give the Boltzmann equilibrium for isothermal electron conditions. The result is consistent since a Maxwellian velocity distribution $(m/(2\pi T_e))^{3/2} \exp(-(\frac{1}{2} m u^2 - e\phi(\mathbf{r}))/T_e)$ with constant T_e is a solution to the collisionless steady-state electron Vlasov equation for any given $\phi(\mathbf{r})$. For the standard version of the Bohm sheath problem, all electrons are assumed to be reflected from the sheath facing a negatively biased conducting surface. For realistic conditions, the most energetic electrons can overcome the negative potential to reach the terminating surface and be lost there. Consequently, the assumed Boltzmann equilibrium is not exact. In the calculations, we mostly use applied potentials $\phi_0 = -2.5 T_e/e$, giving a fraction of absorbed electrons to be small, 1.267×10^{-2} . For $\phi_0 = -5 T_e/e$, the corresponding fraction is even smaller, 7.827×10^{-4} . The assumption of isothermal electrons is justified for a negative end-plate bias $\phi_0 \ll -T_e/e$, although exceptions can be found around the transition from sheath to pre-sheath where the dynamic spatial variations of the electric field are large. For magnetized plasmas (a problem not considered in the present work), such local deviations from an isothermal Boltzmann electron distribution were argued.²⁴ With total reflection from the sheath, the electrons are confined. The absorbed ions are assumed to be replaced from $\zeta \rightarrow \infty$. For finite systems, there have to be internal ion sources. For isothermal electrons and cold ions, the thermal forces²⁵ does not play any role. For more complex systems, they may become important.

In the following, we consider the basic equations (1)–(3) for one-, two-, and three-dimensional problems. A previous study¹⁰ addressed the problem by the method of characteristics. We comment on this method in an Appendix B, mentioning also some of its limitations.

III. SHEATHS AND PRE-SHEATHS IN ONE SPATIAL DIMENSION

Here, we assume that a conducting plate is placed at $x=0$ with the plasma filling the half-space $x > 0$. A negative potential is applied to the plate to attract ions and deflect electrons. In a practical experiment, some of the most energetic electrons in the “tail” of the Maxwellian distribution will reach the end-plate and be lost, implying that the assumed isothermal electron distribution cannot be exact. It is implicitly assumed that the applied potential is sufficiently negative to make the fraction of lost electrons to be negligible.

Using the ion sound speed C_s , the electron Debye length λ_D , and a characteristic perturbation length scale \mathcal{L} , the following normalizations are introduced $\psi = e\phi/T_e$, $\xi = x/\mathcal{L}$, $\tau = C_s t/\mathcal{L}$, $v = u/C_s$, $n/n_p \rightarrow n$, to give the basic equations in the form:

$$\begin{aligned} \frac{\partial}{\partial \tau} v + v \frac{\partial}{\partial \xi} v &= -\frac{\partial}{\partial \xi} \psi, \\ \rightarrow \frac{\partial v}{\partial \tau} &= -\frac{\partial \mathcal{H}}{\partial \xi}, \quad \mathcal{H} = \frac{v^2}{2} + \psi, \end{aligned} \quad (4)$$

$$\frac{\partial}{\partial \tau} n + \frac{\partial}{\partial \xi} (nv) = 0, \quad (5)$$

$$\epsilon \frac{\partial^2}{\partial \xi^2} \psi = e^\psi - n, \quad \epsilon \equiv \left(\frac{\lambda_D}{L} \right)^2. \quad (6)$$

Equations (4) and (5) are rewritten as

$$\left(\frac{\partial}{\partial \tau} + v \frac{\partial}{\partial \xi} \right) v = - \frac{\partial \psi}{\partial \xi}, \quad (7)$$

$$\left(\frac{\partial}{\partial \tau} + v \frac{\partial}{\partial \xi} \right) \ln \left\{ e^\psi - \epsilon \frac{\partial^2 \psi}{\partial \xi^2} \right\} = - \frac{\partial v}{\partial \xi}. \quad (8)$$

The assumption of quasi-neutrality is imposed by setting $\epsilon = 0$ in Eq. (8).

A. Static sheath formation

Static solutions to the basic equations are given by

$$nv = J = n_s v_s, \quad \frac{v^2}{2} + \psi = \mathcal{H} = \frac{v_s^2}{2} + \psi_s, \quad (9)$$

$$nv^2 + e^\psi - \frac{\epsilon}{2} \left(\frac{d\psi}{d\xi} \right)^2 = n_s v_s^2 + e^{\psi_s} - \frac{\epsilon}{2} \left(\frac{d\psi_s}{d\xi} \right)^2,$$

where $n_s = n(\xi_s)$, $v_s = v(\xi_s)$ and $\psi_s = \psi(\xi_s)$ are all evaluated at the sheath edge $\xi = \xi_s$. Poisson's equation now reads

$$\epsilon \frac{d^2 \psi}{d\xi^2} = e^\psi - \frac{J}{\sqrt{2(\mathcal{H} - \psi)}}, \quad (10)$$

which is integrated to give

$$\frac{\epsilon}{2} \left(\frac{d\psi}{d\xi} \right)^2 = \frac{\epsilon}{2} \left(\frac{d\psi}{d\xi} \Big|_{\xi_s} \right)^2 + e^\psi - e^{\psi_s} + J \left(\sqrt{2(\mathcal{H} - \psi)} - \sqrt{2(\mathcal{H} - \psi_s)} \right), \quad (11)$$

where the potential is bounded in the region given by

$$\psi(\xi) \leq \psi_s + \frac{v_s^2}{2}. \quad (12)$$

The relation (11) shows that stationary sheath solutions are possible only when $v_s^2 \geq 1$. This is Bohm's result for a collisionless plasma.

B. Comments on a stationary pre-sheath in one dimension

The sheath and plasma are supposed to be connected smoothly to a quasi-neutral pre-sheath. Then, we set $\epsilon = 0$ ($n = e^\psi$) in Eq. (10) to get

$$e^\psi = \frac{J}{\sqrt{2(\mathcal{H} - \psi)}} = \frac{n_s}{\sqrt{1 - 2(\psi - \psi_s)}},$$

$$\rightarrow e^{\psi - \psi_s} = \frac{1}{\sqrt{1 - 2(\psi - \psi_s)}} \quad (13)$$

with a solution given as

$$\psi(\xi) = \psi_s, \quad (14)$$

implying that the potential in the pre-sheath region is constant and there is no potential drop through the pre-sheath. The ions cannot be

accelerated to the sound speed. This is confirmed as follows. From the equation of motion and the continuity equation, we have

$$v(\xi) \frac{dv(\xi)}{d\xi} = - \frac{d\psi(\xi)}{d\xi}, \quad v(\xi) \frac{d\psi(\xi)}{d\xi} = - \frac{dv(\xi)}{d\xi}, \quad (15)$$

combined to give

$$(v^2(\xi) - 1) \frac{dv(\xi)}{d\xi} = \frac{d}{d\xi} \left\{ \frac{1}{3} v^3(\xi) - v(\xi) \right\} = 0$$

$$\rightarrow v(\xi) \{ v^2(\xi) - 3 \} = \text{const.}, \quad (16)$$

showing that $v(\xi)$ is constant in the assumed pre-sheath and there is thus no ion acceleration. Consequently, no such stationary pre-sheath exists in one spatial dimension. Previous studies^{9,10} found dynamic evolutions similar to those described in our work but did not address the nonexistence of a stationary pre-sheath.

C. Self-similar pre-sheath evolution

By the quasi-neutral condition imposed by setting $\epsilon = 0$ in Eq. (8), there are no characteristic scales length for pre-sheath models. When such scales are absent also in the initial or boundary conditions, we can expect a pre-sheath to be described by self-similar solutions. Physically, a relevant condition will correspond to a sudden disturbance being applied at a reference position in the present one-dimensional model. Imposing a negative potential to absorb ions at a conducting surface, we find a rarefaction wave propagating into the plasma. Such a problem has been studied also experimentally.⁹ We can also have step-like initial conditions in the plasma density¹¹⁻¹⁴ and find self-similar solutions also for this case. For positive parameters λ (not to be confused with the electron Debye length λ_D) and χ , we find the expressions

$$v(\xi, \tau) = w \left(\frac{\xi}{\lambda}, \frac{\tau}{\lambda^a} \right), \quad \psi(\xi, \tau) = \varphi \left(\frac{\xi}{\lambda}, \frac{\tau}{\lambda^b} \right), \quad (17)$$

then we have

$$\left\{ \frac{\partial}{\partial \tau} + \frac{1}{\lambda^{1-a}} w \left(\frac{\xi}{\lambda}, \frac{\tau}{\lambda^a} \right) \frac{\partial}{\partial \xi} \right\} w \left(\frac{\xi}{\lambda}, \frac{\tau}{\lambda^a} \right) = - \frac{\lambda^a}{\chi} \frac{\partial}{\partial \xi} \varphi \left(\frac{\xi}{\lambda}, \frac{\tau}{\lambda^b} \right), \quad (18)$$

$$\left\{ \frac{\partial}{\partial \tau} + \frac{1}{\lambda^{1-b}} w \left(\frac{\xi}{\lambda}, \frac{\tau}{\lambda^a} \right) \frac{\partial}{\partial \xi} \right\} \varphi \left(\frac{\xi}{\lambda}, \frac{\tau}{\lambda^b} \right) = - \frac{\chi^b}{\lambda} \frac{\partial}{\partial \xi} w \left(\frac{\xi}{\lambda}, \frac{\tau}{\lambda^a} \right), \quad (19)$$

which have isomorphism with Eqs. (7) and (8) for $\lambda = \chi$, $a = b = 1$. Putting $\lambda = \tau$, and

$$w = w \left(\frac{\xi}{\tau}, 1 \right) = w(\rho), \quad \varphi = \varphi \left(\frac{\xi}{\tau}, 1 \right) = \varphi(\rho), \quad \rho = \frac{\xi}{\tau},$$

then Eqs. (18) and (19) reduce to

$$\left\{ \frac{\partial \rho}{\partial \tau} + \frac{\partial \rho}{\partial \xi} w(\rho) \right\} \frac{dw(\rho)}{d\rho} = - \frac{\partial \rho}{\partial \xi} \frac{d\varphi(\rho)}{d\rho},$$

$$\left\{ \frac{\partial \rho}{\partial \tau} + \frac{\partial \rho}{\partial \xi} w(\rho) \right\} \frac{d\varphi(\rho)}{d\rho} = - \frac{\partial \rho}{\partial \xi} \frac{dw(\rho)}{d\rho}.$$

Using

$$\frac{\partial \rho}{\partial \tau} = - \frac{\xi}{\tau^2}, \quad \frac{\partial \rho}{\partial \xi} = \frac{1}{\tau},$$

we have

$$(-\rho + w(\rho)) \frac{dw(\rho)}{d\rho} = -\frac{d\varphi(\rho)}{d\rho}, \quad (20)$$

$$(-\rho + w(\rho)) \frac{d\varphi(\rho)}{d\rho} = -\frac{dw(\rho)}{d\rho}, \quad (21)$$

$$n(\rho) = e^{\varphi(\rho)} \quad (22)$$

with ρ being the only independent variable. If $\epsilon \neq 0$ is retained in Eq. (8), this self-similar form is no longer possible. The relations (20)–(22) are combined to give

$$(-\rho + w(\rho))^2 \frac{dw(\rho)}{d\rho} = \frac{dw(\rho)}{d\rho}, \quad \rightarrow w(\rho) = \rho \pm 1 \quad (23)$$

and

$$\frac{d\varphi(\rho)}{d\rho} = \mp 1, \quad \rightarrow \varphi(\rho) = \mp \rho + \varphi(0). \quad (24)$$

Thus, we have for $\xi_s \leq \xi \leq \xi_p$ under the boundary condition $v(\xi_s, \tau) = -1$ and $\psi(\xi_s, \tau)$, where ξ_p and ξ_s are the plasma–pre-sheath boundary and the sheath edge, respectively,

$$v(\xi, \tau) = w(\rho) = \rho - 1, \quad (25)$$

$$\psi(\xi, \tau) = \varphi(\rho) = \rho + \varphi_s, \quad \text{and} \quad \varphi_s = \varphi(\rho_s).$$

With the present variables, the pre-sheath extends from $\rho = 0$ to $\rho = \rho_p$. In the pre-sheath $w(\rho) \neq 0$, while $w(\rho) = 0$ in the unperturbed plasma where the rarefaction wave has not arrived yet. By this geometry, we require $w(\rho_p) = 0$ at the moving pre-sheath front where $\rho = \rho_p$. Thus, we have

$$\rho_p = \frac{\xi_p(\tau)}{\tau} = 1, \quad \rightarrow \xi_p(\tau) = \tau. \quad (26)$$

The potential at the pre-sheath front is given by

$$\varphi(\rho_p) = \varphi_p = \varphi_s + \rho_p = \varphi_s + 1. \quad (27)$$

Therefore, the potential drop along the dynamic, or expanding, pre-sheath is

$$\varphi_s - \varphi_p = -1. \quad (28)$$

The freedom to choose an electrostatic reference potential can be used to take $\varphi_p = 0$. The plasma density is given by

$$n(\rho) = e^{\varphi(\rho)} = n_p e^{\varphi(\rho) - \varphi_p}, \quad (29)$$

giving the density drop over the dynamic pre-sheath as $n_s = n_p e^{-1}$.

Now Eqs. (20) and (21) are rewritten as

$$\frac{d}{d\rho} \left\{ \frac{(w(\rho) - \rho)^2}{2} + \varphi(\rho) \right\} = \rho - w(\rho) = 1$$

$$\rightarrow \frac{d}{d\rho} \left\{ \frac{(w(\rho) - \rho)^2}{2} + \varphi(\rho) - \rho \right\} = 0, \quad (30)$$

which gives with (26)

$$\frac{(w(\rho) - \rho)^2}{2} + \varphi(\rho) - \rho = C = \frac{1}{2} + \varphi_s = \varphi_p - \frac{1}{2}, \quad (31)$$

where C is a constant determined at the sheath edge and the pre-sheath front. The last expression in Eq. (31) gives Eq. (28).

The analysis in this and related studies¹⁰ have one flaw: the condition on the velocity at the pre-sheath edge is imposed as a boundary condition to be the sound speed, whereas all that the Bohm condition prescribes is that this velocity has to be equal to or greater than C_s . As demonstrated later, this velocity has to be exactly the sound speed, i.e., a more strict condition than the one commonly assumed, see also the Appendix B. Inclusion of isothermal ion dynamics gives only trivial modifications to the results.

1. Comments of the potential and density drops for stationary pre-sheaths in one dimension

In a widely accepted static model, the ion velocity and the potential are assumed to vanish at the position separating the main plasma and the pre-sheath (possibly at infinity). Then, the constant C is set to zero in Eq. (31). The potential at the sheath edge is then given by

$$\varphi_s = -\frac{1}{2}. \quad (32)$$

Physically, this means that an ion is accelerated to the sound velocity by the static potential drop. The corresponding electron density at the sheath edge is

$$n_s = e^{\varphi_s} = e^{-1/2} = 0.61 \quad (33)$$

to be interpreted as the density reduction in the pre-sheath since $n_p = 1$ (corresponding to $\varphi_p = 0$) is the plasma density at the interface between the main plasma and the pre-sheath, the plasma density variation assumed to be continuous. (This position may be found at infinity.) However, for $C = 0$, the potential at the pre-sheath front position separating it from the main plasma is given from Eq. (31) by $\varphi_p = 1/2$, leading to

$$n_p = e^{\varphi_p} = e^{1/2} = 1.649 \quad \rightarrow \quad n_s = n_p e^{-1}, \quad (34)$$

which is nothing but (29). Thus, the result for the density drop in the pre-sheath given by Eq. (33) in the stationary model is inconsistent with the dynamic model. Physically, a steady-state model gives the ion acceleration corresponding to the potential drop, while a dynamic model has the electric field to vary during the ion transit. The difference between static and dynamic pre-sheath may appear controversial and is therefore addressed in more detail in the Appendix C.

IV. BOUNDARY CONDITION FOR THE ION VELOCITY AT THE SHEATH EDGE

Guided by the results in Sec. III C as well as in previous works,¹⁰ we postulate a solution in the form of a normalized electric field, $E(\tau) = g(\tau)$, without any length scale, independent of position in some so far unspecified range $0 < \xi < \xi_0$ but depending on time. We can expect that the spatial range is time varying, $\xi_0 = \xi_0(\tau)$. Both signs of g have to be possible, depending on the plasma being at half-space $\xi > 0$ or $\xi < 0$, the criterion being that ions are accelerated toward the absorbing end-plate. Insertion of $E(\tau)$ into Poisson's equation gives the quasi-neutral solution $n = \exp(\psi)$. This excludes the plasma sheath (the inner solution) and the proposed electric field model does not apply there. The normalized electrostatic potential derived from $E(\tau)$ is $\psi(\xi, \tau) = f(\tau) - \xi g(\tau)$, where $f(\tau)$ is possibly a

function of time, unspecified so far. The corresponding normalized quasi-neutral plasma density is $n(\tau, \xi) = \exp(f(\tau) - g(\tau) \xi)$. The assumption of a stationary sheath implies that $n(\tau, 0) = \text{constant}$ for all times, giving $f(\tau) = f_0$ being a constant. Since a region with charge imbalance is not accounted for in the present analytical model, we can take the pre-sheath edge to be $\xi = 0$, which will correspond to a physical position $x \approx 15\lambda_D$. In the limit of quasi-neutral plasmas, the Debye length becomes immaterial.⁵ Since the sheath width scales with λ_D , the difference between $\xi = 0$ and $\xi = 15$ is of no consequence here. The sheath formation time $\sim \lambda_D/C_s$ becomes infinitesimal in the present limit.⁵

Using the expression for the ion density found before in the continuity equation, we find an equation for the ion flow velocity

$$\exp(\psi) \left(\frac{\partial v(\xi, \tau)}{\partial \xi} - \xi g'(\tau) - v(\xi, \tau)g(\tau) \right) = 0,$$

where a common factor $\exp(\psi) = \exp(f_0 - g(\tau) \xi)$ cancels. The general solution for $v(\xi, \tau)$ is

$$v(\xi, \tau) = A(\tau)e^{\xi g(\tau)} - \frac{g'(\tau)(1 + \xi g(\tau))}{g^2(\tau)} \quad (35)$$

with $A(\tau)$ so far unspecified. Using this result in the ion momentum equation, we find the constraint on the functions $A(\tau)$ and $g(\tau)$,

$$e^{\xi g(\tau)} A'(\tau) - \frac{\xi g''(\tau) + 2A(\tau)e^{\xi g(\tau)} g'(\tau)}{g(\tau)} - g(\tau) \left(1 - (A(\tau)e^{\xi g(\tau)})^2 \right) + \frac{3g'(\tau)^2}{g(\tau)^3} + \frac{2\xi g'(\tau)^2 - g''(\tau)}{g(\tau)^2} = 0. \quad (36)$$

For this condition to be fulfilled for all ξ , it is required that $A^2(\tau)e^{2\xi g(\tau)} = 0$,

$$e^{\xi g(\tau)} \left(A'(\tau) - \frac{2A(\tau)g'(\tau)}{g(\tau)} \right) = 0$$

and

$$\xi \left(\frac{2g'(\tau)^2}{g(\tau)^2} - \frac{g''(\tau)}{g(\tau)} \right) = 0,$$

as well as

$$\frac{3g'(\tau)^2}{g(\tau)^3} - g(\tau) - \frac{g''(\tau)}{g(\tau)^2} = 0.$$

The solution of Eq. (36) is found as $A(\tau) = 0$, and $g(\tau) = -1/(\tau + c_1)$, with c_1 being a constant. The choice $c_1 = 0$ gives the self-similar result for the normalized potential $\psi(\xi, \tau) = f_0 + \xi/\tau$. By Eq. (35), the ion velocity becomes $v(\xi, \tau) = -1 + \xi/\tau$ in the spatial range given for the electric field. This solution is consistent with an initial condition for the potential being a “step function.” The corresponding ion density becomes $n(\xi, \tau) = \exp(f_0 + \xi/\tau)$ in the given spatial range. We find $v(0, \tau) = -1$ for $\tau > 0$, corresponding to ions arriving at $\xi = 0$ with a velocity equal to the sound speed. The observation is consistent with our numerical results when we identify this “analytical” boundary position $\xi = 0$ with the position of the sheath edge. The velocity condition found here is sufficient to ensure a stable plasma sheath in the “Bohm sense.”

These results summarized here are exact solutions to the normalized version of the full set of Eqs. (1)–(3) in the assumed spatial interval and fulfill a boundary condition at $\xi = 0$. The requirement $v \leq 0$ limits the spatial range of the solution (and thereby also for the assumed electric field) to be $\tau \geq \xi \geq 0$ in normalized variables so that $\xi_0(\tau) = \tau$. We consequently complete the expressions for velocity, potential, and the electric field by introducing Heaviside’s unit step function $\mathcal{S}(1 - \xi/\tau)$. The point $\xi/\tau = 1$ is singular in the sense that the ion velocities and the electric fields are not differentiable there. The quasi-neutrality assumption breaks down at this position. The singularity in the derivative at $\xi = \tau$ arises from the assumed step-like initial value. For the normalized plasma density, we have $n(\xi \rightarrow \infty, \tau) = 1$ corresponding to the reference density n_p in physical units, implying $n(\xi = \tau) = 1$. Hereby, we obtain $f_0 = -1$ and the analytical solution is fully specified giving, in particular, $n(0) = \exp(-1) \equiv 1/e$.

The imposed potential and resulting electric field at the terminating conducting plate is accelerating ions and thereby increasing the ion kinetic energy. In normalized units, the ion kinetic energy density is $\frac{1}{2}nv^2 = \frac{1}{2}(1 - \xi/\tau)^2 \exp(-1 + \xi/\tau)$ for $0 \leq \xi \leq \tau$. The total kinetic energy per unit area is found as $\tau(1 - 5/(2e)) \approx 0.0803 \tau$. The total ion kinetic energy is unbounded for $\tau \rightarrow \infty$. For realistic physical conditions, the pre-sheath expansion will be arrested by physical boundaries at some finite time.

To address conditions like those met in, for instance Q-machines,^{18,26} we allow for ion inflow from $\xi \rightarrow \infty$ with a normalized subsonic velocity $-U$. In this case, an ion sound wave will propagate in the positive ξ direction with a normalized velocity $1 - U$ and the Heaviside step function introduced before is modified to $\mathcal{S}(1 - U - \xi/\tau)$. The normalized potential solution becomes $\psi(\xi, \tau) = f_0 + \xi/\tau$ now with $f_0 = U - 1$ giving corresponding modifications of $n(\xi, \tau)$, while $v(\xi, \tau) = -1 + \xi/\tau$ remains unchanged. This problem is only relevant for the one-dimensional problem, e.g., along the homogeneous magnetic field in a Q-machine. It does not apply to cylindrically or spherically symmetric problems where a net unidirectional plasma flow will break the assumed symmetry.

A. Distributed ion velocities in one spatial dimension

The foregoing analysis demonstrated the absence of a steady-state pre-sheath in one spatial dimension, assuming cold ions. The following analysis demonstrates that distributed ion velocities do not change this conclusion. The problem can be approached by taking the integration constant in Eq. (7) for steady state to be $\frac{1}{2}V^2$ with V being the incoming ion velocity, where $V = 0$ was a special case implied in the previous result. We can assume that there are several such incoming velocity components with velocities V_j , where $j = 1, 2, \dots$ is a label for velocity groups, each with their separate normalized densities n_j . The individual velocity components evolve according to the local collective electric field $E = -d\varphi/d\xi$. The set of equations for N incoming ion velocity components becomes

$$\frac{1}{2}v_j^2(\xi) + \varphi(\xi) = \frac{1}{2}V_j, \quad (37)$$

found by the ion momentum equation. From the stationary continuity equation, we have

$$n_j(\xi)v_j(\xi) = C_j. \quad (38)$$

The quasi-neutrality condition gives

$$\sum_j^N n_j = \exp(\varphi). \quad (39)$$

The integration constant is recognized as $C_j = n_{0j} V_j$ with n_{0j} being the relative density of the incoming velocity component, with $\sum_j^N n_{0j} = 1$. Proper choice of n_{0j} for $j = 1, 2, \dots$ allows modeling of a velocity distribution, for instance, a Maxwellian.

We can reduce these equations to

$$\exp(\varphi) = \sum_j^N \frac{n_{0j} V_j}{\sqrt{V_j^2 - 2\varphi}}.$$

No matter how dense the velocities of incoming ions are, this equation has no solution in form of a function of ξ that can serve as a spatially varying pre-sheath, not even in the limit of a continuum of incoming ion velocities.²⁷ Ion kinetic effects alone do not suffice to give a stationary pre-sheath in one spatial dimension. Ion Landau damping is a dynamic feature, while collisional friction is effective also for steady-state flow conditions, so the two effects have different consequences. The conclusion remains of course also for $N=1$ confirming the foregoing result concerning the nonexistence of a stationary pre-sheath on one spatial dimension. From the results of present section, we can conclude that a cold ion model suffices to give the basic elements of the sheath-pre-sheath problem so it will be used in the following.

V. COLLISIONAL PRE-SHEATH IN ONE SPATIAL DIMENSION

The basic set of equations in one spatial dimension is generalized by including a standard collision term $-\mu v$ in the ion momentum equation,²⁻⁴ taking the collision frequency μ constant for the moment. The model accounts for momentum losses of ions due to collisions with a heavy neutral background gas, for instance. There is no loss or generation of ions in this model. These latter processes require additional terms in the ion continuity equation and are not considered here. This case is fundamentally different from the collisionless problem since we now have a characteristic length scale in C_s/μ . With the normalizations $\psi = e\phi/T_e$, $\xi = x/L$, $\tau = C_s t/L$, $v = u/C_s$, $n/n_p \rightarrow n$, and $\mu L/C_s \rightarrow \mu$, the basic equations are rewritten as

$$\frac{\partial}{\partial \tau} v + v \frac{\partial}{\partial \xi} v = -\frac{\partial}{\partial \xi} \psi - \mu v, \quad (40)$$

$$\frac{\partial}{\partial \tau} n + \frac{\partial}{\partial \xi} (nv) = 0, \quad (41)$$

$$\epsilon \frac{\partial^2}{\partial \xi^2} \psi = e^\psi - n, \quad \epsilon = \left(\frac{\lambda_D}{L}\right)^2, \quad (42)$$

which are rewritten for a quasi-neutral system ($n = e^\psi$) as

$$\left(\frac{\partial}{\partial \tau} + v \frac{\partial}{\partial \xi}\right) v = -\frac{\partial \psi}{\partial \xi} - \mu v, \quad (43)$$

$$\left(\frac{\partial}{\partial \tau} + v \frac{\partial}{\partial \xi}\right) \psi = -\frac{\partial v}{\partial \xi}. \quad (44)$$

A. Static collisional pre-sheath in one dimension

For a static case, we have

$$v \frac{dv}{d\xi} = -\frac{d\psi}{d\xi} - \mu v, \quad v \frac{d\psi}{d\xi} = -\frac{dv}{d\xi}, \quad (45)$$

leading to

$$\frac{dv}{d\xi} = -\frac{1}{v} \frac{d\psi}{d\xi} - \mu, \quad \rightarrow \frac{d}{d\xi} \left(v + \frac{1}{v} + \mu \xi \right) = 0, \quad (46)$$

$$v \frac{d\psi}{d\xi} = -\frac{dv}{d\xi}, \quad \rightarrow \frac{d}{d\xi} \left(\psi + \frac{1}{2} \ln v^2 \right) = 0, \quad (47)$$

which, with integration constants C_1 and C_2 , give

$$v + \frac{1}{v} + \mu \xi = C_1 = v_s + \frac{1}{v_s} + \mu \xi_s, \quad (48)$$

$$\psi + \frac{1}{2} \ln v^2 = C_2 = \psi_s + \frac{1}{2} \ln v_s^2,$$

where $v_s = v(\xi_s)$, $\psi_s = \psi(\xi_s)$ and $n_s = n(\xi_s)$ are obtained at the sheath edge $\xi = \xi_s$.

Then, we have

$$v(\xi) = \frac{1}{2} \left\{ -(\mu \xi - C_1) + \sqrt{(\mu \xi - C_1)^2 - 4} \right\}, \quad (49)$$

$$\psi(\xi) = C_2 - \frac{1}{2} \ln v^2(\xi)$$

with the two constants C_1 and C_2 being connected by the conditions at $\xi = 0$, giving $C_1 = -(1 + v^2(0))/v(0)$ and $C_2 = \psi(0) + \frac{1}{2} \ln v^2(0)$. We know that $v(0) = -1$ for the collisionless case and expect that ions are slowed down by the collisions (as supported by numerical results). Consequently, $-1 \leq v(0) < 0$ and $\exp(-1) \leq \psi(0) < 1$. For the illustrative choice of boundary conditions at the sheath edge $\xi_s = 0$ to be $v(\xi_s) = v_s = -1$ and $\psi(\xi_s) = \psi_s$, the integration constants become

$$C_1 = -2, \quad C_2 = \psi_s, \quad (50)$$

giving

$$v(\xi) = \frac{1}{2} \left\{ -(\mu \xi + 2) + \sqrt{(\mu \xi + 2)^2 - 4} \right\}, \quad (51)$$

$$\psi(\xi) = \psi_s - \frac{1}{2} \ln v^2(\xi), \quad n(\xi) = e^{\psi(\xi)},$$

where $-1 \leq v(\xi) < 0$ follows for the given conditions. Conservation of flux, $nv = \text{constant}$ by the steady-state continuity equation, implies that the plasma density must diverge when $v \rightarrow 0$ for $\xi \rightarrow \infty$, so the plasma density n becomes infinite there, irrespective of the applied velocity condition at the sheath edge. The ion velocity (full line), the potential (dashed line), and ion density (dash-dotted-line) in the collisional pre-sheath for varying $\mu \xi$ are shown in Fig. 1 for the assumed condition giving $v(0) = -1$. The electrostatic potential vanishes here for $\mu \xi_s = e^{1/2} + e^{-1/2} - 2 \approx 0.255$, and $n(\xi_s) = 1$ there. The potential is unbounded as $\mu \xi \rightarrow \infty$, just as the plasma density. The electric field is negative for all $\xi > 0$ but diverging for $\xi \rightarrow 0$. This divergence is problematic only if we take the pre-sheath position literally. In reality, this point is defined only to the accuracy of λ_D . As a conclusion, we have demonstrated that a steady-state solution exists for the chosen collision model, but find that this cannot be a global solution

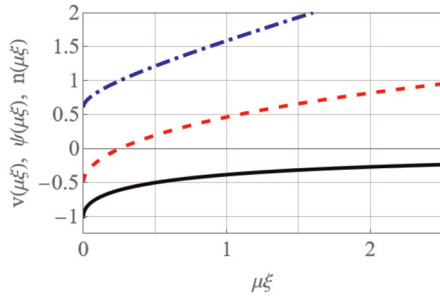


FIG. 1. Illustrations of analytical results for the ion velocity (full line), the potential (dashed line), and ion density (dash-dotted-line) in the collisional pre-sheath for varying $\mu\xi$ for the choice of constants (50). The velocity derivative is singular at $\xi = 0$ in agreement with Eq. (52) for the assumed velocity condition at $\xi = 0$. The condition was chosen to illustrate the divergence of the velocity derivative for $v = -1$.

approached asymptotically by physically acceptable boundary and/or initial conditions. Just as the collisionless case, also this model has to be solved as an initial value problem irrespective of the existence of a stationary solution.

1. Velocity-dependent collision frequencies

The foregoing Sec. V assumed a simple constant collision frequency μ , independent of velocity. Albeit simple, it is a physically realizable model, at least in a finite velocity range for “Maxwellian molecules.”²⁸ We there find for a wide particle velocity range the cross section $\sigma(u) \sim 1/u$ giving $\mu(u) \sim \text{constant}$.²⁹ This model is widely used for illustrations of the effects of collisional processes.⁴ It can model ion collisions with heavy neutrals, for instance. More detailed studies are reported in the literature.^{2,21}

More generally, the collision frequency will depend on the relative velocity u between the scattered and the scattering particle. Since all ions have the same velocity in the present cold ion model, the particle velocity will here be the same as the ion fluid velocity v .

Taking here a more general case with $\mu = \mu(v)$, we combine the expressions (45) and (47) to give the form²

$$\frac{dv}{d\xi} = \frac{\mu(v)v^2}{1-v^2}, \quad (52)$$

demonstrating that the velocity derivative is singular for $v = \pm 1$, which in the present normalized variables correspond to the velocity being equal to the Bohm velocity $\sqrt{T_e/M} = C_s$. The spatial velocity derivative will have a constant sign as long as $-1 \leq v \leq 1$, relevant here and apply just as well for the case where the plasma is placed at the negative ξ side of the conducting surface. An asymptotically constant velocity for $\xi \rightarrow \infty$ cannot be made consistent with Eq. (52), implying that $v(\xi \rightarrow \infty) = 0$ is the only acceptable solution. The consequence of this velocity variation is that the density $n(\xi) \sim 1/v(\xi)$ is diverging as $\xi \rightarrow \infty$. This will be so for any $\mu(v) \neq 0$, implying that the results from the previous Sec. V A are robust. The arguments here are independent of imposed boundary conditions and will apply also

for finite systems bounded by two surfaces, not necessarily on the same bias.

Physically, the present results mean that a finite pressure gradient $T_e dn(\xi)/d\xi$ is needed at $\xi \rightarrow \infty$ to overcome the frictional drag on the ions, so they can arrive at the biased end-plate and be absorbed there. This gradient in density gives rise to the divergence $n(\xi \rightarrow \infty) \rightarrow \infty$. For an initial value problem with an expanding rarefaction wave, this problem does not exist in one spatial dimension.

We have not found analytical solutions $v = v(\xi)$ for the present case. From Eq. (52), we can find an the inverse expression $\xi = \xi(v)$ in an integral form for given $\mu(v)$,

$$\xi(v) = \int_{-a}^v \frac{1-K^2}{\mu(K)K^2} dK, \quad (53)$$

assuming a boundary condition $v = -a$ for $\xi = 0$. The inversion to give $v(\xi)$ can be made graphically. For special model choices of $\mu(K)$, it can be possible to solve (53) analytically. The collisionless case gave the result $v = -1$ at the pre-sheath edge irrespective of the sheath conditions, i.e., applied potentials ψ_0 . Collisional friction will slow the ions down, implying that the collisionless result is approximate and useful only when $C_s/\mu \gg \lambda_D$, i.e., the collisional mean free path is much larger than the sheath width. The requirement $dv(\xi)/d\xi = 0$ imposes constraints on the numerator of Eq. (53).

The collision model with constant μ used in the first part of this Sec. V is relatively simple. More general models are available,³⁰ with classical viscosity already mentioned. The present model serves to demonstrate that a steady-state pre-sheath can be found as soon as a parameter with dimension *length* can be formed that determines the width of a pre-sheath. Such a solution will not, however, necessarily be physically relevant as a global solution for the present one-dimensional case.

2. Plasma sources and sinks

We found that the problem with divergences of density and potential was associated with the continuity equation which in steady state gives $n \sim 1/v$. A more general model with spatially distributed plasma sources with a constant intensity G has been suggested² to give $d(nv)/d\xi = G$ in steady state. This expression is however not consistent with the requirement of a constant ion flux nv at $\xi \rightarrow \infty$. We can generalize the steady-state ion continuity equation to

$$\frac{d(nv)}{d\xi} = \alpha n - \beta n^2, \quad (54)$$

with $\alpha > 0$ and $\beta > 0$ being coefficients for ionization and recombination,² or alternatively keep G instead of αn . The source of ionization in Eq. (54) is taken to be impact on neutrals by fast electrons³¹ and proportional to their density n_e , which becomes n by the assumption of quasi-neutrality. The energy lost to ionization has to be replaced by internal energization. The term accounting for losses is here assumed to represent 3-body recombination, being proportional to the product $n_e n_i$, which becomes n^2 by quasi-neutrality. There are other models for sources, e.g., a simple constant,² while losses can be caused by radiative or by dissociative recombination.³¹ The asymptotic condition $d(nv)/d\xi = 0$ here implies $n = \alpha/\beta$ by Eq. (54). We have a lengthy implicit expression for the ion velocity, but this is not given here. Seemingly, it can only be solved by numerical methods.

For finite one-dimensional systems with two boundaries or with internal length scales, it is generally possible to find steady-state solutions when sources are included to compensate the ion losses to the biased conducting surfaces. In such cases it is, however, the experimental system and not the plasma parameters that sets the scale sizes of the pre-sheath.

VI. CYLINDRICAL CO-ORDINATES

In the one-dimensional sheath and pre-sheath model, it is natural to consider the sheath as well as the biased conducting surface to be a perfect absorber. The equivalent problem in two or three spatial dimensions can be interpreted in terms of a biased Langmuir probe in sheath or in orbit limited conditions.² For the first one of these, we can take the sheath to be a perfect absorber, but it imposes restrictions on a characteristic length, such as the probe radius, as $R \gg \lambda_D$.

Transform from a rectangular co-ordinate system to a cylindrical co-ordinate system: $(x, y, z) \rightarrow (r, \theta, z)$. Keeping here only the radial variations, the basic equations are found in the form

$$\frac{\partial v_r}{\partial \tau} + v_r \frac{\partial v_r}{\partial r} = -\frac{\partial \psi}{\partial r}, \quad (55)$$

$$\frac{\partial n}{\partial \tau} + \frac{\partial n v_r}{\partial r} + \frac{n v_r}{r} = 0, \quad (56)$$

$$\epsilon \left\{ \frac{1}{r} \frac{\partial}{\partial r} \left(r \frac{\partial}{\partial r} \right) + \frac{\partial^2}{\partial z^2} \right\} \psi = e^\psi - n, \quad (57)$$

to be analyzed in the following, where we let r_s be the radius of the conducting surface.

A. Static axisymmetric sheaths

In the following relations, we consider an axisymmetric system:

$$\begin{aligned} \frac{1}{2} \frac{\partial}{\partial r} v_r^2 &= -\frac{\partial \psi}{\partial r}, \\ \frac{1}{r} \frac{\partial}{\partial r} (r n v_r) &= 0, \\ \epsilon \frac{1}{r} \frac{\partial}{\partial r} \left(r \frac{\partial \psi}{\partial r} \right) &= e^\psi - n. \end{aligned}$$

Somewhat more general conditions will have the radial forces balanced by the centrifugal force and the energy gradient in the radial direction. In the present case, a relation for the ion density is

$$n = n_s \frac{r_s v_{rs}}{r v_r} = \frac{n_s r_s v_{rs}}{\sqrt{v_{rs}^2 r^2 + 2r^2(\psi_s - \psi)}}, \quad (58)$$

and Poisson's equation becomes

$$\epsilon \frac{1}{r} \frac{\partial}{\partial r} \left(r \frac{\partial \psi}{\partial r} \right) = e^\psi - \frac{n_s r_s v_{rs}}{\sqrt{v_{rs}^2 r^2 + 2r^2(\psi_s - \psi)}}. \quad (59)$$

We have then

$$\begin{aligned} \epsilon \frac{1}{r} \frac{\partial}{\partial r} \left(r \frac{\partial \psi}{\partial r} \right) &= e^\psi - \frac{n_s r_s v_{rs}}{r \sqrt{v_{rs}^2 + 2(\psi_s - \psi)}} \\ &\simeq n_s \left\{ \left(1 - \frac{r_s}{r} \right) + \left(v_{rs}^2 - \frac{r_s}{r} \right) \frac{\psi - \psi_s}{v_{rs}^2} + \dots \right\}, \quad (60) \end{aligned}$$

where $n_s = e^{\psi_s}$. The solution is given by a modified Bessel function in the vicinity of $r \simeq r_s$ for $|v_{rs}| > \sqrt{r_s/r} \sim 1$, which corresponds to the Bohm criterion for a stable sheath structure to exist for collisionless plasmas in a two-dimensional cylindrically symmetric system.

VII. SPHERICAL CO-ORDINATES

We take a three-dimensional case with co-ordinates $(x, y, z) \rightarrow (r, \phi, \theta)$. For a spherically symmetric case with radial variations only, i.e., $\partial/\partial\theta = 0$ and $\partial/\partial\phi = 0$ and vanishing azimuthal and poloidal velocities, $v_\theta = 0$ and $v_\phi = 0$, we have

$$\frac{\partial v_r}{\partial \tau} + v_r \frac{\partial v_r}{\partial r} = -\frac{\partial \psi}{\partial r}, \quad \rightarrow \quad \frac{\partial v_r}{\partial \tau} = -\frac{\partial}{\partial r} \left(\frac{v_r^2}{2} + \psi \right), \quad (61)$$

$$\frac{\partial n}{\partial \tau} + \frac{1}{r^2} \frac{\partial (r^2 n v_r)}{\partial r} = 0,$$

$$\rightarrow \left(\frac{\partial}{\partial \tau} + v_r \frac{\partial}{\partial r} \right) \ln n + \frac{\partial v_r}{\partial r} + \frac{2v_r}{r} = 0, \quad (62)$$

$$\epsilon \frac{1}{r^2} \frac{\partial}{\partial r} \left(r^2 \frac{\partial \psi}{\partial r} \right) = e^\psi - n. \quad (63)$$

The quasi-neutral limit is also here found for $\epsilon = 0$. For this case, we have no expression corresponding to Eq. (60).

A. Combined expressions for cylindrical and spherical cases

For strictly symmetric cylindrical and spherical symmetries, it is possible to combine the basic equations to a compact form by introducing a modified ion density as $N \equiv r n$ and $N \equiv r^2 n$, respectively, for the two cases. These symmetries are restrictive, but relevant since many plasma probes are constructed with these symmetries. Introducing the dimensionality of the problem as D , we find with a little effort

$$\frac{\partial v_r}{\partial \tau} = -\frac{\partial}{\partial r} \left(\frac{v_r^2}{2} + \psi \right), \quad (64)$$

$$\frac{\partial N}{\partial \tau} + \frac{\partial (N v_r)}{\partial r} = 0, \quad (65)$$

$$\epsilon \frac{\partial}{\partial r} \left(r^{D-1} \frac{\partial \psi}{\partial r} \right) = r^{D-1} e^\psi - N. \quad (66)$$

For $D = 1$, the expressions include also the spatially one-dimensional case. This set of equations is particularly useful for solutions for static pre-sheaths in the two special cases.

B. Static pre-sheaths, analytical results

The steady-state solution, in particular, is found by the set of equations

$$\frac{1}{2} v^2(r) + \psi(r) = C_1$$

$$N(r) v(r) = C_2$$

$$N(r) = r^{D-1} \exp(\psi(r)),$$

where N and ψ can be eliminated to give

$$\frac{1}{2}v^2 + \ln C_2 - \ln v - (D - 1) \ln r = C_1.$$

The solution of this expression valid for $D = 2, 3$ is found in terms of the “ProductLog” or “Lambert’s \mathcal{W} ” function as

$$U(r) = \pm \mathcal{R}e \left\{ i \sqrt{\mathcal{W}(-C_2^2 e^{-2C_1} r^{2-2D})} \right\}, \quad (67)$$

where the constants C_1 and C_2 are determined by the conditions at the surface at $r = 1$ in units normalized by the radius r_s of the surface. Since $N(r) = r^{D-1}n(r) \rightarrow \infty$ at $r \rightarrow \infty$, those boundary conditions are of no use here. For $D = 1$, we have a false solution for v in Eq. (67), consistent with our previous results for one spatial dimension. The result (67) is shown in Fig. 2 together with results for density and potential derived from it. Numerical results for a spherical probe obtained by assuming isothermal electrons as in the present study extended by kinetic “particle-in-cell” (PIC) model for the ions²³ show a radial plasma density variation for the pre-sheath similar to our results.

For the analysis to be meaningful, it was implicitly assumed that $r_s \gg \lambda_D$ so that the spherical surface acts as a sheath limited and not an orbit limited probe. The velocity v is here a fluid velocity, not an individual particle velocity. Since the sheath width scales as $\sim \lambda_D$, it is here immaterial whether the boundary condition is imposed at a position $r = r_s$ or at $r \approx r_s + \lambda_D$.

The width of a saturated pre-sheath scale linearly with r_s . A characteristic time for its establishing is r_s/C_s . For short times, a locally plane approximation is useful and there the one-dimensional dynamic sheath results apply. The characteristics of the sheath itself are almost indistinguishable from the one-dimensional case when $r_s \gg \lambda_D$.

As for the one-dimensional case, the electric field induced by the applied potential accelerates ions also here. Recalling $\mathcal{W}(\zeta^{-n}) \sim \zeta^{-n}$ for $\zeta \rightarrow \infty$, it is readily demonstrated that the total kinetic ion energy

is finite for the spherically symmetric case for all times, and similarly for the cylindrical case for a segment of unit length along the z axis.

VIII. NUMERICAL RESULTS

A. Time evolution of one-dimensional collisionless sheaths and pre-sheaths

Early previous studies⁹ analyzed the expanding sheath by numerical solutions of the basic equations, using the computer resources available at the time. The present results are obtained by a commercially available program. The spatial length of the systems is usually taken to be $10^3 \lambda_D$ in physical units. The accuracy of the results has been confirmed in part by comparison with analytical results when available, and also by tests using larger spatial domains, e.g., double size or larger. The figures in the following show only a part of the spatial calculation domain. Concerning the time durations, we usually show all time-steps obtained. A typical calculation time is $300/\Omega_{pi}$ in physical units. A rarefaction wave excited by the initial condition propagates into the plasma with the ion sound speed $C_s = \sqrt{T_e/M}$ and its front will reach approximately 1/3 of the calculation domain within a calculation time. Reflections from the terminating end are not an issue.

After normalizations, the full set of the combined nonlinear equations (1)–(3) is solved numerically with results shown in Figs. 3–6. The boundary condition assumes an externally applied normalized potential ψ_0 at the terminating surface absorbing the ions at $\zeta = 0$. After a short time where the sheath itself is established, Figs. 3 and 4 show a steady expansion of the pre-sheath. Based on Figs. 5 and 6, we can conclude that for collisionless plasma conditions, the pre-sheath expands at a constant rate with the ion sound speed. The sheath itself is established in a short time, a few ion plasma periods, and remains stationary from then on. These results have experimental support.⁹

The sheath is found to be fully developed at a time $\sim 10/\Omega_{pi}$ with negligible changes after $\sim 50/\Omega_{pi}$. For the collisionless case, the transition from sheath to pre-sheath can be identified as the point where

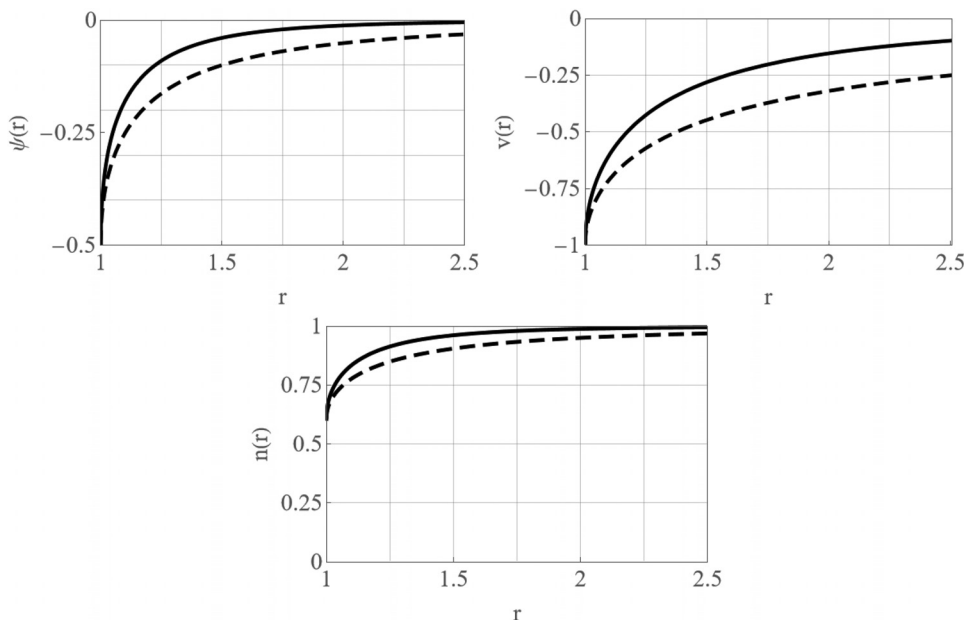


FIG. 2. Exact analytical results for the steady-state collisionless pre-sheath solutions for potential, velocity and density in the three-dimensional spherically symmetric case (full lines) and the two-dimensional cylindrical case (dashed lines). The potential and density drops are noticeably different from the one-dimensional dynamic case. The normalizing constants are here chosen so that $r = 1$ corresponds to $r_s \gg \lambda_D$.

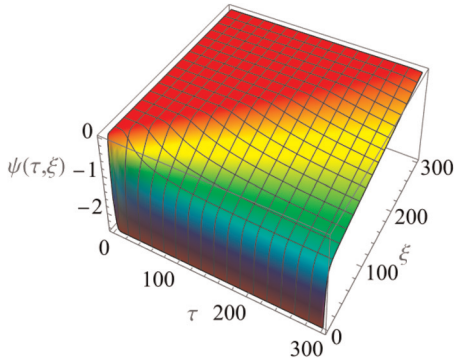


FIG. 3. Space–time evolution of the normalized electrostatic potential for $\psi_0 = -2.5$ for the collisionless case in one spatial dimension without quasi-neutrality assumed. The figure shows the rarefaction wave propagating at the ion sound speed in the positive ξ -direction.

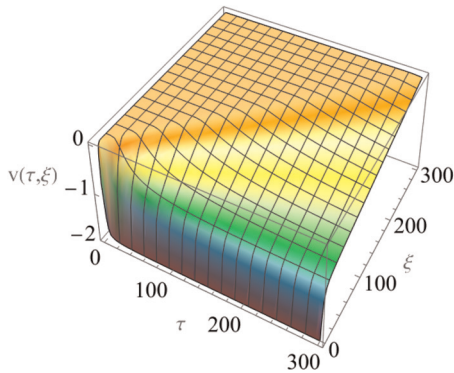


FIG. 4. Space–time evolution of the normalized ion velocity for an applied potential of $\psi_0 = -2.5$, corresponding to Fig. 3. Different color schemes were used for potential and velocity to avoid confusion.

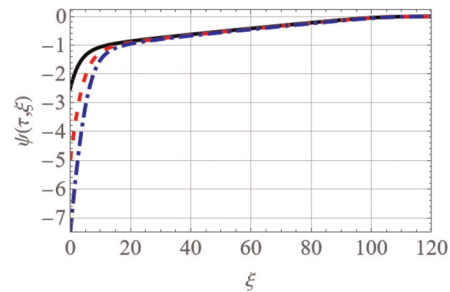


FIG. 5. Spatial variation of the normalized electrostatic potential $\psi(\xi, \tau)$ for $\psi_0 = -2.5, -5,$ and -7.5 , shown with full, dashed, and dot-dashed lines for the collisionless case. The results are taken at a time $\tau = 100$, where the rarefaction wave has reached the position $\xi = 100$.

quasi-neutrality is reached, here at $\xi \approx 15$. Other definitions of the sheath edge have been proposed, however.³² Our arguments for defining the sheath edge are based on the observation that for a collisionless system described by our basic equations taken in the quasi-neutral limit, our analysis demonstrates that the arrival ion velocity at the pre-

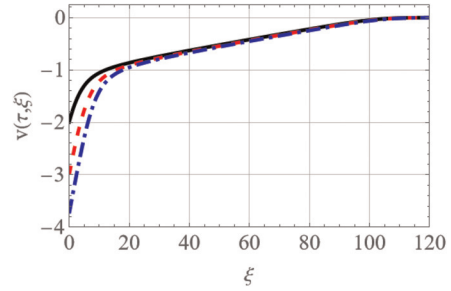


FIG. 6. Spatial variation of the normalized ion velocity $v(\xi, \tau)$ for $\psi_0 = -2.5, -5.0,$ and -7.5 taken at a time $\tau = 100$ as in Fig. 5 with full, dashed, and dot-dashed lines. Compare with Figs. 4 and 5. The edge of the pre-sheath is here identified, approximately, as the position where $\psi \approx -1$ and simultaneously $v \approx -1$, here at $\xi \approx 15$.

sheath edge is exactly the sound speed for the collisionless case. Then, for the full numerical solution, without the restriction of quasi-neutrality, we take the separation point to be the position where the velocity takes the value of the sound speed. By inspection of our figures for collisionless conditions, this position turns out to be very close to the point we would have chosen visually without any prior information. The separation point moves for varying ψ_0 , but less than a factor of 2 for the given parameter range. To a good approximation, the electrostatic potential reaches a value $\psi \approx -1$ at the position of the sheath boundary. It is the same position where the ion velocity reaches $v \approx -1$, i.e., the sound speed. The numerical solutions demonstrate that the ion velocity at the sheath edge evolves self-consistently to become $v_s = -1$ in normalized units, i.e., the sound speed, and not imposed as a boundary condition.

To keep the model in its original classical form, we did not include finite ion thermal effects. Inclusion of isothermal ions at temperature $T_i > 0$ is simple, both numerically and analytically. It amounts to a redefinition of the sound speed to be $C_s = \sqrt{(T_e + T_i)/M}$ and does not contribute with anything new. Adiabatic ion models will be important for the internal sheath solutions³³ and are not considered here. The analytical results for the pre-sheath are independent of the applied potential ψ_0 , indicating that the main plasma containing the pre-sheath is completely shielded from the terminating plate. Consequently, the pre-sheath evolution is expected to be insensitive to slow potential oscillations added to ψ_0 . For the oscillations to be “slow,” the period has to be longer than the $\sim 10/\Omega_{pi}$ that it takes to establish the plasma sheath. This feature is confirmed numerically. For density variations due to incoming ion sound waves, for instance, the situation is different.

The results shown in Figs. 5 and 6 demonstrate that the pre-sheath dynamics are to a good approximation independent of the bias ψ_0 of the terminating conducting plane surface. The sheath width is seen to increase when the end-plate bias is made more negative. Calculations assuming adiabatic ions at a large temperature ratio (here $T_e/T_i = 10$) give results for the pre-sheath that are nearly indiscernible from the corresponding isothermal ion results. Differences are found in the sheath close to the biased surface. Other studies³⁴ have indicated that a simple adiabatic ion model can be questionable here.

B. Collisional pre-sheath in one dimension

The ion momentum equation (1) is modified to include collisional effects in the form μv , with μ being a normalized collision

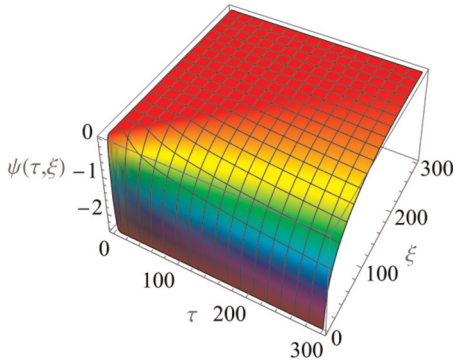


FIG. 7. Space–time evolution of the normalized electrostatic potential for a normalized collision frequency $\mu = 1/25$ and $\psi_0 = -2.5$ for the one-dimensional case. Compare with the collisionless results in Fig. 3.

frequency. It is demonstrated by numerical results in Fig. 7 that this change gives significant modifications of the collisionless results.^{35,36} Most important is that for large collision frequencies μ , the steady-state pre-sheath expansion is arrested and the system saturates in a quasi-stationary configuration, with pre-sheath width scaling as C_s/μ . Note that a classical viscosity term in the form $\mu \partial^2 v/\partial x^2$, with μ being a kinetic viscosity, has an effect only near the beginning and end points, $\xi = 0$ and $\xi_0 = \tau$, respectively, of the pre-sheath, since the original velocity variation is to a good approximation linear between these two points. The numerical solutions giving Fig. 7 assume the physically reasonable reference plasma potential $\phi_p = 0$ in the unperturbed plasma. The steady increase in potential for $\xi \rightarrow \infty$ in Fig. 1 is not found. The change in the plasma parameters induced by changing the collision frequency is shown in more detail in Fig. 8 for two collision frequencies. For a small μ , there is only little difference from the collisionless case, while strong collisionality gives a pronounced effect on the spatial variation of velocity and ion density, less for the potential. In particular, we still have $\phi \approx -1$ at the sheath edge. For $\mu > 1/5$, also the potential is affected and its value at the sheath edge will decrease in absolute value. Recall here that the potential is fixed at the conducting end-plate by the applied potential ψ_0 .

We find that the time evolution follows the collisionless case for a short time interval, up to $\sim 10/\mu$. After this, the time evolution saturates to give a sheath that is nearly stationary within the computational time, see Fig. 7 illustrating a case with a moderate collision frequency. The pre-sheath remains insensitive to changes in the applied potential ψ_0 as it was for $\mu = 0$. Due to the collisional drag, the ions here arrive to the terminating plate at a velocity that is smaller than the value in the collisionless case, see Fig. 8. The pre-sheath width is approximately constant at a length $\sim 10 C_s/\mu$. The figure illustrates that the ions arrive the sheath edge as well as the terminating surface at $\xi = 0$ with a reduced velocity for increasing collisionality. For $C_s/\mu \gg \lambda_D$, implying that the collisional mean free path is larger than the sheath width, the reduction in velocity is inconspicuous, however. That ions arrive to the sheath at a reduced velocity, which makes the definition of the sheath to pre-sheath transition point ambiguous.

Detailed collisional fluid models have been analyzed,^{37,38} including thermal forces, heat fluxes, and collisional temperature isotropization for both electrons and ions. The results were supported by kinetic simulations. These studies present spatial variations only without time

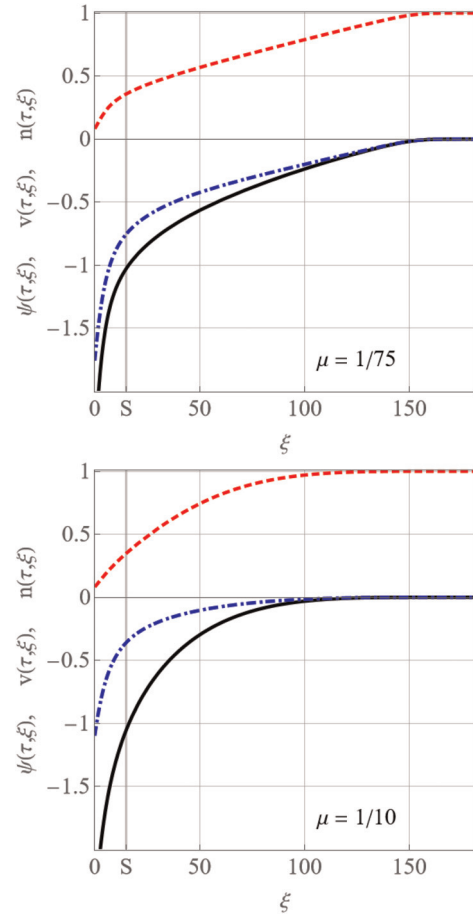


FIG. 8. Spatial variation of the normalized electrostatic potential, velocity, and ion density for a normalized collision frequencies $\mu = 1/75$ and $1/10$, both for a fixed time $\tau = 150$ for the one-dimensional case. We have $\psi_0 = -2.5$. Full black line is for potential, dot-dashed blue line for velocity, and red dashed line for ion density. A vertical gray line marked “S” gives the approximate position of the sheath edge. Compare also with the collisionless results in Fig. 3. The curves for velocity and potential coincide in the pre-sheath for the collisionless case, $\mu = 0$.

variations leading to those spatial variations. It is not possible to make detailed comparisons with our results, but we note that the basic features presented there are similar to what we find at late times in our much simpler models.

C. Time evolution of collisionless sheaths and pre-sheaths in spherical geometry

Numerical results for initial value conditions are shown in Figs. 9 and 10. The spatial variable is here normalized with λ_D , and the radius of the biased conducting sphere is $r_s = 50\lambda_D$ to have $r_s \gg \lambda_D$. The sheath thickness is found to be $\sim 10\lambda_D$ for this case. Contrary to the one-dimensional case, we find that after a transient phase, the solutions reach a quasi-stationary limit, which is well accounted for by the analytical solutions, see Fig. 2. The time evolution in the initial phase, where the sheath thickness is much less than r_s , is well described $r_s \sim \lambda_D$ the one-dimensional model in Sec. III. Here, the sheath can be

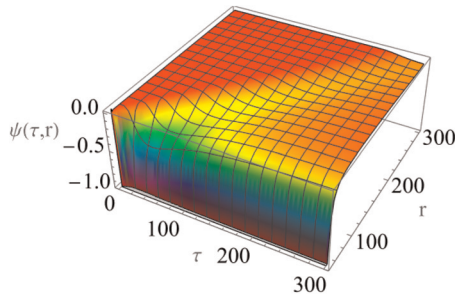


FIG. 9. Space–time evolution of the normalized electrostatic potential in spherical geometry for $\psi_0 = -2.5$. The spatial variable is here normalized with λ_D , and the radius of the biased conducting sphere is $r_s = 50\lambda_D$. Only a part of the vertical axis is shown.

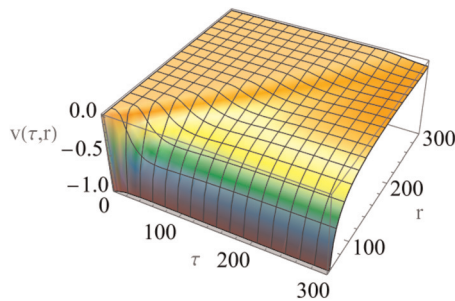


FIG. 10. Space–time evolution of the normalized ion velocity in spherical geometry for an applied potential of $\psi_0 = -2.5$, corresponding to Fig. 9. Different color schemes were used for potential and velocity also here to avoid confusion.

seen as a thin layer covering the spherical surface. Conditions are different when $r_s \sim \lambda_D$, which is not covered by the present analysis. The same arguments apply for the cylindrical case.

The accuracy of the analytical results in Fig. 2 is here illustrated by a comparison for the velocity, see Fig. 11. There is a small freedom in merging the two curves at the sheath position, which is not given exactly. The analytical solution is slightly above the numerical result, which is taken from a late stage of the dynamical evolution, the

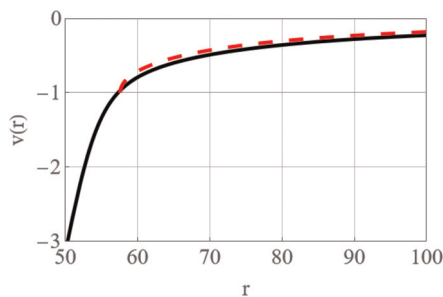


FIG. 11. Comparison of the numerical solution in Fig. 10 for the spherical case, here sampled at $\tau = 200$ (full line) and the analytical solution for velocity in Fig. 2 (dashed line). The two curves are merged at the sheath edge, here defines as the position where $v = -1$. The radius of the spherical surface is here $R = 50$. The agreement is similar for the two-dimensional cylindrical case.

difference accommodated by the time derivative in the evolution equation. The agreement is fully satisfactory, and similar for potential and density. Deviations are found at the sheath edge where the analysis predicts a vertical derivative, where the numerical solutions, as expected, give a differentiable transition from pre-sheath to sheath.

D. Spherical geometry with ion collisions

Introducing a collision frequency, the steady-state basic equations become in normalized form

$$\frac{1}{2} \frac{d}{dr} v^2(r) = -\frac{d}{dr} \psi(r) - \mu v(r) \tag{68}$$

with μ being a normalized collision frequency. The continuity equation becomes

$$\frac{d}{dr} (r^2 n(r) v(r)) = 0. \tag{69}$$

Using these expressions together with the quasi-neutral expression $n = \exp(\psi)$, we use Eq. (68) to arrive at a relation with Boltzmann distributed electrons

$$\frac{1}{2} \frac{d}{dr} v^2(r) = -\frac{d}{dr} \ln(n(r)) - \mu v(r). \tag{70}$$

From Eq. (69), we have $n = C_1 / (r^2 v(r))$ and find

$$\frac{1}{2} \frac{d}{dr} v^2(r) = -\frac{d}{dr} \ln\left(\frac{C_1}{r^2 v(r)}\right) - \mu v(r). \tag{71}$$

There seems to be no analytical solution for this equation, but a solution exists. We can solve the full set of equations where Poisson’s equation is included, allowing for a charge imbalanced sheath. Results for the velocity variation are shown in Fig. 12 for a selected collisional case. For a short time, smaller than the collision time, the velocity evolves almost like a collisionless case, see Fig. 10, until it asymptotically approaches a semi-stationary limit.

IX. CONCLUSION

The standard reference model for deriving the Bohm criterion requires the formation of a pre-sheath needed for accelerating ions to the sound speed or more at the sheath edge. While the sheath itself possesses a characteristic length scale, the Debye length, λ_D , for

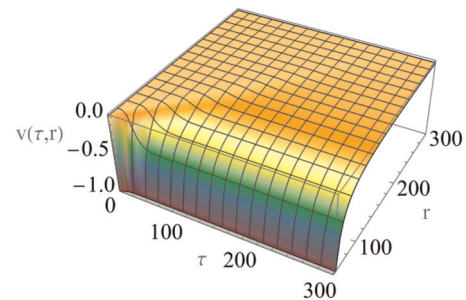


FIG. 12. Space–time evolution of the normalized ion velocity in spherical geometry for an applied potential of $\psi_0 = -2.5$ and a normalized collision frequency of $\mu = 1/50$.

normalization, the quasi-neutral pre-sheath has no characteristic parameter of dimension length available for normalization. Assuming a high temperature ratio plasma, $T_e/T_i \gg 1$, we propose a solution of this puzzle by considering the sheath evolution as an initial value problem, giving a steadily expanding pre-sheath, with no characteristic fixed length scale. The ion flow velocity reaches the ion sound value in a short time (a few ion plasma periods) after application of the bias. The fact that it takes a long time (infinitely long, for ideal conditions) for the pre-sheath to be formed will not have implications for the interpretation of the current signal to a plasma probe, not even with a slowly varying bias²³ since the ion flow velocity at the sheath edge is constant at the sound speed after a few ion plasma periods. One conclusion of the present analysis, analytical as well as numerical, is that after the pre-sheath acceleration, the ions arrive at the sheath edge with the sound speed and not some arbitrary velocity equal to or larger than this value.

The analytical results for the quasi-neutral pre-sheaths in two and three dimensions show that the spatial derivatives of potential, velocity and plasma density are diverging at the sheath edge. The electric fields are infinite at this point. This unphysical result is a consequence of assigning a precise position for the separation between sheath and pre-sheath. As seen in the full solutions allowing for deviations from quasi-neutrality shown in Figs. 3–11, this transition is gradual and the separation point is determined to the accuracy of λ_D . This inaccuracy is localized to a narrow spatial region as seen best in Fig. 11. The analytical results found for collisionless cylindrical and spherical geometries agree with those being standard for steady state acceleration potentials.

Conditions in laboratory or in numerical simulations contain a characteristic length scale, the system size, and this will arrest the expansion of a one-dimensional pre-sheath. Also, a collisional mean free path will serve as a characteristic length scale,^{2,39} as discussed also in the present Sec. V. In magnetized plasmas, the Larmor radius introduces a new length scale,^{17,24,40} but these conditions are not considered here. For experimentally achievable plasma conditions, the electron temperature ratios will have some finite ratio and Landau damping will be effective.⁴¹ The ion Landau damping of the rarefaction wave front will be dominating the electron Landau damping for moderate and small temperature ratios.

The first part of the present analysis was restricted to the classical version of the Bohm sheath problem with a plane conducting surface at a constant negative bias, see Sec. III. The conditions are different from what is found for a floating surface, which is not considered here. Most experiments in laboratory or in space have a geometry that can be approximated either by a cylindrical or a spherical geometry. The radial potential variation will depend of the specific geometry and not solely by plasma parameters. These problems were addressed in Secs. VI and VII. Realizable analytical solutions could be found for these cases. The observations in Sec. V A demonstrated that the mere existence of an analytical solution does not guarantee that it can be reached by physically realistic or realizable initial conditions.

It is found that for given imposed conditions the two- and three-dimensional pre-sheath problems have a static as well as a dynamic solution, where we presented analytical forms for the static limits and numerical solutions for the dynamic evolution. These static solutions form natural limiting or saturated stages for the dynamic evolutions. The one-dimensional problem has only a dynamic self-similar solution with a derivation presented here and also argued by dimensional reasoning. The potential drop along this time-evolving solution differs

notably from what would be expected for a postulated static solution. It was explicitly demonstrated that no such static solution exists for this problem. A previous study¹⁰ also arrived at the dynamic solution, but did not prove that it is the only one. A collisional case in one dimension was analyzed but found to be peculiar by offering an inaccessible steady-state analytical solution. The dynamic solution for this case could be found only by numerical analysis. It is possible that the analytical steady-state solutions can find use for a finite system bounded by two biased conducting surfaces. We have not explored this possibility.

The problem can find applications also for fusion experiments: if we follow a magnetic field line starting from a diverter in a tokamak geometry, the one-dimensional model can be used as an approximation.⁴² Sheaths will develop at the conducting surfaces, and the pre-sheaths expand until they reached the core plasma where the plasma losses are compensated by plasma production. This will then be the characteristic distance determining the length scale of the steady-state problem. There will be an electric field component along these magnetic field lines. Any density perturbation injected in this region by for instance transport across magnetic field lines will be accelerated, rather than be dispersing as a sound wave perturbation.

Studies extending the results summarized in this paper can be based on numerical kinetic plasma simulations as well as complete plasma transport models.^{23,37,38} They will provide extensions of our analysis, but have to contain the results of the present study as a limiting case. Complex conditions with collisional plasmas with excitation and recombination in inhomogeneous magnetic fields^{2,43} probably need to be studied by numerical simulations.

ACKNOWLEDGMENTS

We thank Professor Alexander Piel for valuable comments on collisional pre-sheaths.

AUTHOR DECLARATIONS

Conflict of Interest

The authors have no conflicts to disclose.

Author Contributions

Mitsuo Kono: Conceptualization (equal); Formal analysis (equal); Methodology (equal); Software (equal); Writing – original draft (supporting); Writing – review & editing (equal). **Hans L. Pécseli:** Conceptualization (equal); Formal analysis (equal); Methodology (equal); Software (equal); Writing – original draft (lead); Writing – review & editing (equal).

DATA AVAILABILITY

Data sharing is not applicable to this article as no new data were created or analyzed in this study.

APPENDIX A: DIMENSIONAL REASONING

The dimension matrix for the present problem is given by Table I. The density is from the outset normalized everywhere by the reference density n_p to form a dimensionless variable, so that n_p appears explicitly only through Poisson's equation. The ion mass is here denoted M_i to be distinguished from the dimension "mass" given by the letter M .

TABLE I. Temperature T_e is given in energy units, incorporating Boltzmann's constant. The physical parameters of the problem, here with cold ions, are n_p , M_i , e , ε_0 , T_e , and R together with the externally applied potential ϕ_0 . By choice of reference, we have here the plasma potential $\phi_p = 0$. The dimensions in the first column are denoted by T(ime), L(ength), M(ass), and A(mper) for current.

	t	x	u	ϕ	n_p	M_i	e	ε_0	T_e	R	ϕ_0
T	1	0	-1	-3	0	0	1	4	-2	0	-3
L	0	1	1	2	-3	0	0	-3	2	1	2
M	0	0	0	1	0	1	0	-1	1	0	1
A	0	0	0	-1	0	0	1	2	0	0	-1

If we search a time-stationary solution, we ignore the first column. Studying a quasi-neutral limit, we discard the column containing ε_0 . In this case, the density can be normalized by n_p everywhere, so the reference density n_p becomes obsolete. Consequently, we can omit also the corresponding column. For the present one-dimensional pre-sheath model, there is no length scale of the problem, and consequently, we omit the column for R .

Any physically acceptable solution of a problem can be written in the form of a product of a constant having the physically correct dimension and a dimensionless function of one or more dimensionless variables.^{8,44,45} We can, as an example, write for the spatial variation of the stationary ion velocity $U = [U]F(\xi)$, where $F(\xi)$ is a dimensionless function of a dimensionless spatial variable $\xi = x/L$, while $[U]$ is some dimensionally correct constant and L is a length scale. We can choose $e\phi_p/T_e$ and ϕ_p/ϕ_0 as fixed dimensionless constants for the given plasma conditions. Other constants can be formed, but these are not independent. Given the remaining system parameters M_i , e , and T_e , we can form a quantity having dimension of velocity, i.e., $C_s = \sqrt{T_e/M_i}$ the sound speed, but it is not possible to form any "length," so $F(\xi)$ cannot be constructed: there is no steady-state quasi-neutral solution. If the problem has a characteristic length scale, we retain the column for R in Table I and the system parameters become M_i , e , T_e , and R . We can then form a steady-state velocity solution like $u(r) = C_s F(r/R)$, where R can be the radius of a probe in two or three spatial dimensions, or possibly the length scale of a finite size system in one spatial dimension. For the steady-state sheath solution, we have $u(r) = C_s F(r/\lambda_D, \lambda_D/R, e\phi_0/T_e)$, where λ_D/R and $e\phi_0/T_e$ are dimensionless constants for the problem. In either case (two or three dimensions), the function F has to be determined by analysis or by numerical solutions. To account for the full space-time dynamics in the absence of any length scale, e.g., a one dimensional system of infinite extent, the only dimensionally correct combination of variables and parameters is the self-similar solution for velocity $u(x/t) = C_s F(x/C_s t)$ discussed in Sec. III. For the present problem, we found $u(x, t) = x/t$ in the interval $0 < x < C_s t$, i.e., the sound speed enters through the dynamic boundary conditions.

APPENDIX B: PRE-SHEATH FORMATION DERIVED BY CHARACTERISTICS

Pre-sheath solutions are given by

$$\left(\frac{\partial}{\partial \tau} + v(\xi, \tau) \frac{\partial}{\partial \xi}\right) v(\xi, \tau) = -\frac{\partial \psi(\xi, \tau)}{\partial \xi}, \quad (\text{B1})$$

$$\left(\frac{\partial}{\partial \tau} + v(\xi, \tau) \frac{\partial}{\partial \xi}\right) \psi(\xi, \tau) = -\frac{\partial v(\xi, \tau)}{\partial \xi}. \quad (\text{B2})$$

The expressions (B1) and (B2) are combined to yield

$$\begin{aligned} \left(\frac{\partial}{\partial \tau} + v \frac{\partial}{\partial \xi}\right) v &= -\frac{\partial \psi}{\partial \xi}, \quad \rightarrow \quad \frac{\partial v}{\partial \tau} + \frac{\partial \psi}{\partial \xi} = -v \frac{\partial v}{\partial \xi}, \\ \left(\frac{\partial}{\partial \tau} + v \frac{\partial}{\partial \xi}\right) \psi &= -\frac{\partial v}{\partial \xi}, \quad \rightarrow \quad \frac{\partial \psi}{\partial \tau} + \frac{\partial v}{\partial \xi} = -v \frac{\partial \psi}{\partial \xi}. \end{aligned}$$

$$\begin{aligned} \left(\frac{\partial}{\partial \tau} + \frac{\partial}{\partial \xi}\right) (v + \psi) + v \frac{\partial}{\partial \xi} (v + \psi) &= 0, \\ \rightarrow \quad \frac{\partial u_+}{\partial \tau} + (v + 1) \frac{\partial u_+}{\partial \xi} &= 0, \end{aligned} \quad (\text{B3})$$

$$\begin{aligned} \left(\frac{\partial}{\partial \tau} - \frac{\partial}{\partial \xi}\right) (v - \psi) + v \frac{\partial}{\partial \xi} (v - \psi) &= 0, \\ \rightarrow \quad \frac{\partial u_-}{\partial \tau} + (v - 1) \frac{\partial u_-}{\partial \xi} &= 0, \end{aligned} \quad (\text{B4})$$

where $u_+(\xi, \tau) = v(\xi, \tau) + \psi(\xi, \tau)$, and $u_-(\xi, \tau) = v(\xi, \tau) - \psi(\xi, \tau)$. The two expressions $u_+(\xi, \tau)$ and $u_-(\xi, \tau)$ are constant on the characteristics C_+ and C_- defined, respectively, by

$$\begin{aligned} C_+ : \frac{d\xi}{d\tau} &= v(\xi, \tau) + 1, \quad \xi(0) = \xi_s, \\ \rightarrow \quad \xi(\tau) &= \xi_s + \int_0^\tau \{v(\xi(\tau), \tau) + 1\} d\tau, \\ C_- : \frac{d\xi}{d\tau} &= v(\xi, \tau) - 1, \quad \xi(0) = \xi_s, \\ \rightarrow \quad \xi(\tau) &= \xi_s + \int_0^\tau \{v(\xi(\tau), \tau) - 1\} d\tau, \end{aligned} \quad (\text{B5})$$

where ξ_s is the position separating sheath and pre-sheath. Noting

$$\begin{aligned} u_+(\xi(\tau), \tau) &= v_+(\xi, \tau) + \psi_+(\xi, \tau) = u_+(\xi_s, 0) \\ &= v_+(\xi_s, 0) + \psi_+(\xi_s, 0), \quad \text{on } C_+, \\ u_-(\xi(\tau), \tau) &= v_-(\xi, \tau) + \psi_-(\xi, \tau) = u_-(\xi_s, 0) \\ &= v_-(\xi_s, 0) + \psi_-(\xi_s, 0), \quad \text{on } C_-, \end{aligned} \quad (\text{B6})$$

we have

$$\begin{aligned} v(\xi, \tau) &= \begin{cases} v_+(\xi_s, 0) = v_+ & \text{on } C_+ \\ v_-(\xi_s, 0) = v_- & \text{on } C_- \end{cases}, \\ \psi(\xi, \tau) &= \begin{cases} \psi_+(\xi_s, 0) = \psi_+ & \text{on } C_+ \\ \psi_-(\xi_s, 0) = \psi_- & \text{on } C_- \end{cases}. \end{aligned} \quad (\text{B7})$$

From Eq. (B5), we find with $v_\pm = v(\xi_s, 0)$ being the initial conditions at the sheath edge

$$\begin{aligned} C_+ : \xi(\tau) &= \xi_s + (v_+ + 1)\tau, \\ C_- : \xi(\tau) &= \xi_s + (v_- - 1)\tau. \end{aligned} \quad (\text{B8})$$

Then, $v(\xi, \tau)$ and $\psi(\xi, \tau)$ are expressed by the initial condition $v(\xi_s, 0)$ as

$$v(\xi, \tau) = \begin{cases} v(\xi - (v_- - 1)\tau, 0) & \text{on } C_- \\ v(\xi - (v_+ + 1)\tau, 0) & \text{on } C_+ \end{cases}$$

$$\psi(\xi, \tau) = \begin{cases} \psi(\xi - (v_- - 1)\tau, 0) & \text{on } C_- \\ \psi(\xi - (v_+ + 1)\tau, 0) & \text{on } C_+ \end{cases}$$

The slopes of these characteristics are $v_{\pm} \rightarrow \pm 1$, and we may assume $v_+ + 1 > v_- - 1$ for which the solutions are given by

$$v(\xi, \tau) = \begin{cases} v(\xi - (v_- - 1)\tau, 0), & \text{for } \xi - \xi_0 \leq (v_- - 1)\tau, \\ v(\xi - (v_+ + 1)\tau, 0), & \text{for } (v_+ + 1)\tau \leq \xi - \xi_0, \end{cases} \quad (B9)$$

$$\psi(\xi, \tau) = \begin{cases} \psi(\xi - (v_- - 1)\tau, 0), & \text{for } \xi - \xi_0 \leq (v_- - 1)\tau, \\ \psi(\xi - (v_+ + 1)\tau, 0), & \text{for } (v_+ + 1)\tau \leq \xi - \xi_0. \end{cases}$$

These two characteristics separate in a $\xi - \tau$ space, and there remains a region where the characteristics do not cover, that is,

$$(v_- - 1)\tau < \xi - \xi_0 \leq (v_+ + 1)\tau. \quad (B10)$$

and a smooth function to cover the region has to be obtained, see Fig. 13. Since the characteristics are linear in a (ξ, τ) space, we may look for a self-similar solution in a form

$$v(\xi, \tau) = w\left(\frac{\xi}{\tau}\right) = w(\rho), \quad (B11)$$

$$\psi(\xi, \tau) = \varphi\left(\frac{\xi}{\tau}\right) = \varphi(\rho),$$

then Eqs. (B1) and (B2) reduce to

$$(-\rho + w(\rho)) \frac{dw(\rho)}{d\rho} = -\frac{d\varphi(\rho)}{d\rho}, \quad (B12)$$

$$(-\rho + w(\rho)) \frac{d\varphi(\rho)}{d\rho} = -\frac{dw(\rho)}{d\rho}, \quad (B13)$$

which are combined to give

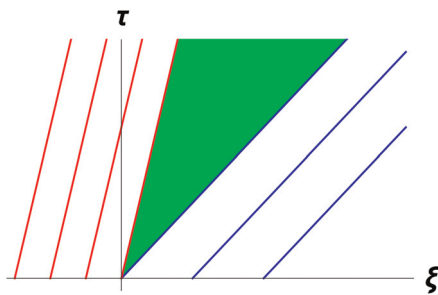


FIG. 13. The shaded region (green) is for not covered by characteristics, i.e., self-similar solution for Eq. (25). Regions with thin lines (blue) are for $C_+ : \xi(\tau) = \xi_0 + (v_+ + 1)\tau$, while (red) is for $C_- : \xi(\tau) = \xi_0 + (v_- - 1)\tau$ for the case of $v_+ + 1 > v_- - 1$.

$$(-\rho + w(\rho))^2 \frac{dw(\rho)}{d\rho} = \frac{dw(\rho)}{d\rho},$$

giving : $w(\rho) = \rho \pm 1$ (B14)

and

$$\frac{d\varphi(\rho)}{d\rho} = \mp 1, \quad \rightarrow \quad \varphi(\rho) = \mp \rho + \varphi_s. \quad (B15)$$

We have for $\xi_s \leq \xi \leq \xi_p$ with ξ_p being the separation between the main plasma and the pre-sheath

$$v(\xi, \tau) = w\left(\frac{\xi - \xi_s}{\tau}\right) = \frac{\xi - \xi_s}{\tau} - 1, \quad (B16)$$

$$\psi(\xi, \tau) = \frac{\xi - \xi_s}{\tau} + \psi_s.$$

The ion velocity at the sheath edge thus automatically gives the Bohm criterion $v(\xi_s, \tau) = -1$. We obtain the solution over all of the range $\xi_0 \leq \xi \leq \xi_p$ as

$$v(\xi, \tau) = \begin{cases} v(\xi - (v_- - 1)\tau, 0), & \text{for } \xi - \xi_0 \leq (v_- - 1)\tau \\ \frac{\xi - \xi_s}{\tau} - 1, & \text{for } (v_- - 1)\tau \leq \xi - \xi_0 < (v_+ + 1)\tau \\ v(\xi - (v_+ + 1)\tau, 0), & \text{for } (v_+ + 1)\tau \leq \xi - \xi_0, \end{cases} \quad (B17)$$

$$\psi(\xi, \tau) = \begin{cases} \psi(\xi - (v_- - 1)\tau, 0), & \text{for } \xi - \xi_0 \leq (v_- - 1)\tau \\ \frac{\xi - \xi_s}{\tau} + \psi_s, & \text{for } (v_- - 1)\tau \leq \xi - \xi_0 < (v_+ + 1)\tau \\ \psi(\xi - (v_+ + 1)\tau, 0), & \text{for } (v_+ + 1)\tau \leq \xi - \xi_0. \end{cases} \quad (B18)$$

The characteristic lines (B8) are shown in Fig. 3.

APPENDIX C: DETAILS ON THE EXPANDING PRE-SHEATH IN ONE SPATIAL DIMENSION

Here is offered another view on the expanding sheath for one spatial dimension with particular attention to the density and potential drops along the dynamic pre-sheath.

Assume that we have a region with an electric field expanding in the positive ξ direction with some constant normalized velocity $U > 0$. The electric field is assumed to decay in time as $\sim 1/t$. Introducing Heaviside's unit step function $S(x)$, we can write the space-time varying electric field in one spatial dimension as

$$E(\xi, \tau) = -\frac{E_0}{\tau} S(U\tau - \xi), \quad (C1)$$

where $E_0 > 0$ is some field amplitude and $\xi > 0$.

Take now an ion representing a small cold plasma fluid element placed initially at rest at a position $X < 0$. Upon the arrival of the electric field front at time $\tau = X/U$, the ion will be accelerated from then on to have a time evolution of its velocity

$$v(\tau) = -E_0 \log(\tau) + E_0 \log(X/U) \\ = -E_0 \log(\tau/(X/U)) \quad \text{for } \tau > X/U. \quad (C2)$$

The position of this ion at times $\tau > X/U$ will then be

$$\xi(\tau) = -E_0(-\tau + \tau \log(\tau) \\ - \tau \log(X/U) + X/U) + X, \\ = -E_0\left(-\tau + \tau \log\left(\frac{\tau}{X/U}\right) + X/U\right) + X. \quad (C3)$$

The time τ_0 where this ion reaches $\xi = 0$, the edge of the pre-sheath, is found by $\xi(\tau = \tau_0) = 0$. The solution in terms of Lambert's \mathcal{W} -function is

$$\tau_0 = -\frac{X(U - E_0)}{E_0 U \mathcal{W}\left(-\frac{U - E_0}{eE_0}\right)} \quad (C4)$$

with e here being Euler's number. By Eq. (C2), the magnitude of the ion velocity at this time, i.e., when it crosses the sheath boundary, is then in terms of the natural logarithm

$$|v(\tau_0)| = E_0 \log\left(\frac{E_0 - U}{E_0 \mathcal{W}\left(\frac{E_0 - U}{eE_0}\right)}\right) \quad (C5)$$

independent of X , i.e., it does not matter where the ion starts, the crossing velocity at $\xi = 0$ will always be the same $v(\tau_0)$.

The two constants E_0 and U are so far undetermined. Concerning U , we note that for large times, the field amplitude becomes small, so that linear theory applies, giving $U = 1$, i.e., the ion sound speed in these normalized units. Since we have U to be a constant, its magnitude has to be the sound speed everywhere.

The plasma is unperturbed for $\xi > U\tau = \tau$, giving $\psi(\xi \rightarrow \infty) = 0$ by our choice of reference potential. Similarly, we have for the normalized density $n(\xi \rightarrow -\infty) = 1$ corresponding to the unperturbed physical density n_p . The expression (C1) for E gives the potential

$$\psi(\xi, \tau) = \left(f_0 - \frac{\xi}{\tau} E_0\right) \mathcal{S}(\xi - \tau) \quad \text{for } \xi/\tau \neq 1, \quad (C6)$$

where f_0 is a constant. The condition for continuous $\psi(\xi, \tau)$ at $\xi = \tau$ gives $f_0 = E_0$ for any finite τ . The corresponding normalized plasma density is $n(\xi, \tau) = \exp(\psi(\xi, \tau))$.

We recall the series expansion of $\mathcal{W}(z)$ for small z to be $\mathcal{W}(z) \approx z - z^2 + \mathcal{O}(z^3)$. Using these expressions, we find that $|v(\tau_0)| \rightarrow 1$ for $E_0 \rightarrow 1$ as required for a stable sheath according to the Bohm criterion. All ions arrive at the sheath edge with exactly the sound speed for $E_0 = 1$. For this case, we find the normalized potential drop from $\xi = \tau$ to $\xi = 0$ to be $\Delta\psi = -1$. The corresponding normalized density drop becomes $\Delta n = \exp(-1) \approx 0.37$.

REFERENCES

¹D. Bohm, "Minimum ionic kinetic energy for a stable sheath," in *The Characteristics of Electric Discharges in Magnetic Field*, edited by A. Guthry and R. K. Wakerling (McGraw-Hill, New York, 1949).
²M. A. Lieberman and A. J. Lichtenberg, *Principles of Plasma Discharges and Materials Processing*, 2nd ed. (John Wiley & Sons, Inc., New York, 2005).

³F. F. Chen, *Introduction to Plasma Physics and Controlled Fusion*, 3rd ed. (Springer, Heidelberg, 2016).
⁴A. Piel, *Plasma Physics: An Introduction to Laboratory, Space, and Fusion Plasmas*, 2nd ed. (Springer, Heidelberg, 2017).
⁵A. Caruso and A. Cavaliere, "The structure of the collisionless plasma-sheath transition," *Il Nuovo Cimento* (1955–1965) **26**, 1389–1404 (1962).
⁶S. D. Baalrud, B. Scheiner, B. T. Yee, M. M. Hopkins, and E. Barnat, "Interaction of biased electrodes and plasmas: Sheaths, double layers, and fireballs," *Plasma Sources Sci. Technol.* **29**, 053001 (2020).
⁷V. Godyak and N. Sternberg, "On the consistency of the collisionless sheath model," *Phys. Plasmas* **9**, 4427–4430 (2002).
⁸E. Buckingham, "On physically similar systems; illustrations of the use of dimensional equations," *Phys. Rev.* **4**, 345–376 (1914).
⁹M. Widner, I. Alexeff, W. D. Jones, and K. E. Lonngren, "Ion acoustic wave excitation and ion sheath evolution," *Phys. Fluids* **13**, 2532–2540 (1970).
¹⁰C. H. Su, "Comments on 'Ion acoustic wave excitation and ion sheath evolution,'" *Phys. Fluids* **14**, 1817–1818 (1971).
¹¹A. L. Gurevich, L. I. Pariiskaya, and L. P. Pitaevskii, "Self similar motion of rarefied plasma," *J. Exp. Theor. Fiz. (U.S.S.R.)* **49**, 647–654 (1965); see also *Sov. Phys. JETP* **22**, 449–454 (1966).
¹²A. L. Gurevich, L. I. Pariiskaya, and L. P. Pitaevskii, "Self similar motion of a low-density plasma. II," *Zh. Eksp. Teor. Fiz.* **54**, 891–904 (1968); see also *Sov. Phys. JETP* **27**, 476–482.
¹³P. Michelsen and H. L. Pécseli, "Propagation of density perturbations in a collisionless Q-machine plasma," *Phys. Fluids* **16**, 221–225 (1973).
¹⁴M. Widner, I. Alexeff, and W. D. Jones, "Plasma expansion into a vacuum," *Phys. Fluids* **14**, 795–796 (1971).
¹⁵S. A. Andersen, G. B. Christoffersen, V. O. Jensen, P. Michelsen, and P. Nielsen, "Measurements of wave-particle interaction in a single ended Q-machine," *Phys. Fluids* **14**, 990–998 (1971).
¹⁶V. L. Rekaa, H. L. Pécseli, and J. K. Trulsen, "Self-similar space-time evolution of an initial density discontinuity," *Phys. Plasmas* **20**, 072117 (2013).
¹⁷S. Basnet, A. Maskey, A. Deuja, and R. Khanal, "Numerical investigation of sheath characteristics for electronegative magnetized plasma and dust charging," *Phys. Plasmas* **28**, 083705 (2021).
¹⁸R. W. Motley, *Q Machines* (Academic Press, New York, 1975).
¹⁹R. J. Taylor, K. R. MacKenzie, and H. Ikezi, "A large double plasma device for plasma beam and wave studies," *Rev. Sci. Instr.* **43**, 1675–1678 (1972).
²⁰R. N. Franklin and J. R. Ockendon, "Asymptotic matching of plasma and sheath in an active low pressure discharge," *J. Plasma Phys.* **4**, 371–385 (1970).
²¹T. E. Sheridan and J. Goree, "Collisional plasma sheath model," *Phys. Fluids B* **3**, 2796–2804 (1991).
²²S. Tskhakaya, D. D. L. Kos, and D. Tskhakaya, "Stability of the Tonks-Langmuir discharge pre-sheath," *Phys. Plasmas* **23**, 032128 (2016).
²³K. M. Kjølberbakken, W. J. Miloch, and K. Roed, "Sheath formation time for spherical Langmuir probes," *J. Plasma Phys.* **89**, 905890102 (2023).
²⁴D. D. Tskhakaya, P. K. Shukla, B. Eliasson, and S. Kuhn, "Theory of the plasma sheath in a magnetic field parallel to the wall," *Phys. Plasmas* **12**, 103503 (2005).
²⁵S. I. Braginskii, "Transport processes in a plasma," in *Reviews of Plasma Physics*, edited by M. A. Leontovich (Consultants Bureau, 1965) Vol. 1, pp. 205–311.
²⁶S. Kuhn, "Determination of axial steady-state potential distributions in collisionless single-ended Q-machines," *Plasma Phys.* **21**, 613–626 (1979).
²⁷J. Dawson, "On Landau damping," *Phys. Fluids* **4**, 869–874 (1961).
²⁸B. A. Trubnikov, "Particle interactions in fully ionized plasmas," in *Reviews of Plasma Physics*, edited by M. A. Leontovich (Consultants Bureau, New York, 1965), Vol. 1, pp. 105–204.
²⁹G. Bekefi, *Radiation Processes in Plasmas* (John Wiley and Sons, New York, 1966).
³⁰N. A. Krall and A. W. Trivelpiece, *Principles of Plasma Physics* (McGraw-Hill, New York, 1973).
³¹R. J. Goldston and P. H. Rutherford, *Introduction to Plasma Physics* (Institute of Physics Publishing, Bristol and Philadelphia, 1995).
³²N. Sternberg and V. Godyak, "The Bohm plasma-sheath model and the Bohm criterion revisited," *IEEE Trans. Plasma Sci.* **35**, 1341–1349 (2007).
³³N. Jelić, K.-U. Riemann, T. Gyergyek, S. Kuhn, M. Stanojević, and J. Duhovnik, "Fluid and kinetic parameters near the plasma-sheath boundary for finite Debye lengths," *Phys. Plasmas* **14**, 103506 (2007).

- ³⁴S. Kuhn, K.-U. Riemann, N. Jelić, S. Tskhakaya, D. D. J. Tskhakaya, and M. Stanojević, "Link between fluid and kinetic parameters near the plasma boundary," *Phys. Plasmas* **13**, 013503 (2006).
- ³⁵K.-U. Riemann, "The influence of collisions on the plasma sheath transition," *Phys. Plasmas* **4**, 4158–4166 (1997).
- ³⁶K.-U. Riemann, "Kinetic analysis of the collisional plasma-sheath transition," *J. Phys. D* **36**, 2811 (2003).
- ³⁷Y. Li, B. Srinivasan, Y. Zhang, and X.-Z. Tang, "Bohm criterion of plasma sheaths away from asymptotic limits," *Phys. Rev. Lett.* **128**, 085002 (2022).
- ³⁸Y. Li, B. Srinivasan, Y. Zhang, and X.-Z. Tang, "Transport physics dependence of Bohm speed in presheath-sheath transition," *Phys. Plasmas* **29**, 113509 (2022).
- ³⁹K.-U. Riemann, "The Bohm criterion and sheath formation," *J. Phys. D* **24**, 493–518 (1991).
- ⁴⁰Z. Guo and X.-Z. Tang, "Parallel transport of long mean-free-path plasmas along open magnetic field lines: Plasma profile variation," *Phys. Plasmas* **19**, 082310 (2012).
- ⁴¹X.-Z. Tang and Z. Guo, "Kinetic model for the collisionless sheath of a collisional plasma," *Phys. Plasmas* **23**, 083503 (2016).
- ⁴²P. C. Stangeby, *The Plasma Boundary of Magnetic Fusion Devices* (CRC-Press, Boca Raton, 2000).
- ⁴³S. Shinohara, *High-Density Helicon Plasma Science, from Basics to Applications*, Springer Series in Plasma Science and Technology (Springer, Singapore, 2022).
- ⁴⁴M. J. Beran, *Statistical Continuum Theories, Monographs in Statistical Physics and Thermodynamics* (Interscience, New York, 1968), Vol. 9.
- ⁴⁵S. Chandrasekhar, "The theory of turbulence," *J. Madras Univ. B* **27**, 251–275 (1957).